Supporting Information

Hydrogen bonding to hexafluoroisopropanol controls the oxidative strength of hypervalent iodine reagents

Ignacio Colomer,[†] Christopher Batchelor-McAuley,[‡] Barbara Odell,[†] Timothy J. Donohoe*[,†] and Richard G. Compton*[,‡]

†Department of Chemistry, Chemistry Research Laboratory, University of Oxford, Mansfield Road, Oxford OX1 3TA, United Kingdom
‡ Department of Chemistry, Physical and Theoretical Chemistry Laboratory, University of Oxford, South Parks Road, Oxford OX1 3QZ, United Kingdom
E-mail: timothy.donohoe@chem.ox.ac.uk
E-mail: richard.compton@chem.ox.ac.uk

Table of Contents

1. General experimental details **S4**

1.1. General procedure for the synthesis of alkenes **S4**

2. Cyclic voltammetry **S5**

2.1. *trans*-Anethole oxidation in ACN **S6**

2.2. *trans*-Anethole oxidation in HFIP **S7**

2.3. PIDA reduction in ACN **S8**

2.4. PIDA reduction in HFIP **S9**

2.5. Ferrocene reference potential in HFIP **S10**

2.6. Voltammetric characterisation of the alkenes in both ACN and HFIP **S10**

2.7. Voltammetric characterisation of iodine(III) reagents PIFA and HTIB in both ACN and HFIP **S14**

3. Mass Spectrometry experimental details **S15**

3.1. HRMS of PIDA **S16**

3.2. HRMS of HFIP **S17**

3.3. HRMS of a 1:1 mixture of HFIP:PIDA **S17**

4. NMR experimental details **S18**

4.1. ^{1}H and ^{13}C NMR of PIDA **S19**

4.2. ^{1}H and ^{13}C NMR of HFIP **S21**

4.3. ^{1}H, ^{13}C NMR, NOESY-2D and nOe of a 1:1 mixture of HFIP:PIDA **S22**

4.4. Comparison table of ^{1}H and ^{13}C NMR for PIDA **S24**

4.5. ^{1}H and ^{13}C NMR of PIFA **S25**

4.6. ^{1}H, ^{13}C NMR, ^{19}F and HOESY of a 1:1 mixture of HFIP:PIFA **S26**

4.7. ^{1}H and ^{13}C NMR of HTIB **S28**

4.8. ^{1}H and ^{13}C NMR of a 1:1 mixture of HFIP:HTIB **S29**

4.9. ^{1}H-DOSY and Diffusion coefficient of PIDA **S30**

4.10. ^{1}H-DOSY and Diffusion coefficient of HFIP **S31**

4.11. ^{1}H-DOSY and Diffusion coefficient of a 1:1 mixture of HFIP:PIDA **S32**

4.12. ^{1}H-DOSY and Diffusion coefficient of *i*-PrOH **S33**

4.13. ^{1}H-DOSY and Diffusion coefficient of a 1:1 mixture of *i*-PrOH:PIDA **S34**

4.14. Table 1. Diffusion coefficients of PIDA (2), *i*-PrOH and the 1:1 mixture of PIDA: *i*-PrOH (6) in $CDCl_3$ as measured via DOSY **S34**

4.15. ^{1}H-DOSY and Diffusion coefficient of PIFA **S35**

4.16. ^{1}H-DOSY and Diffusion coefficient of a 1:1 mixture of HFIP:PIFA **S36**

4.17. Table 2. Diffusion coefficients of PIFA, HFIP and the 1:1 mixture of PIFA:HFIP in $CDCl_3$ as measured via DOSY **S36**

4.18. ^{1}H-DOSY and Diffusion coefficient of HTIB **S37**

4.19. ^{1}H-DOSY and Diffusion coefficient of a 1:1 mixture of HFIP:HTIB **S38**

4.20. Table 3. Diffusion coefficients of HTIB, HFIP and the 1:1 mixture of HTIB:HFIP in $CDCl_3$ as measured via DOSY **S38**

5. References **S39**

1. General experimental details

PIDA, PIFA, HTIB and DMP obtained from Fluorochem were used directly as supplied. HFIP obtained from Flurochem was distilled over activated 4A MS prior to use. $CDCl_3$ obtained from Sigma-Aldrich was treated with K_2CO_3 to neutralize acidic traces, and was stored over activated 4A MS. *trans*-Anethole (**1**) and *trans*-β-methylstyrene (**14**) obtained from Sigma-Aldrich, and *E*-asarone (**6**) obtained from TCI were used directly as supplied.

All voltammetric measurements were recorded using an Autolab PGSTAT30 computer-controlled potentiostat (Metrohm, Utrecht, The Netherlands). Experiments were performed in a Faraday cage using a three-electrode set-up. A platinum mesh was used as the counter electrode and either a glassy carbon macroelectrode (BASi, West Lafayette, IN, USA radius = 1.5 mm) or a carbon fibre microelectrode (ALS electrode supplied by IJ Cambria Scientific , UK, radius = 3.5 μm) were used as the working electrode. The reference electrode was either a silver wire (Goodfellow, UK) acting as a pseudo reference or alternatively for some studies in HFIP a Ag/Ag^+ reference electrode was fabricated and used. The Ag/Ag^+ reference electrode consisted of a pipette with a glass frit filled with 10 mM silver hexfluorophosphate and 0.1 M Bu_4NPF_6 solution in HFIP into which a clean silver wire was submerged. Due to the sensitivity of Ag^+ salts to light the reference electrode was remade daily. Renewal of the working electrode surface was achieved by polishing with alumina slurries in the size sequence 1.0 μm, 0.3 μm and 0.05 μm, (Buehler Ltd, USA). The working electrode was dried under a flow of nitrogen prior to use in the electrochemical experiments. Finally the electrochemical cell was thermostated using a water bath to 25.0±0.3ºC.

1.1. General procedure for the synthesis of *E*-styrenes.

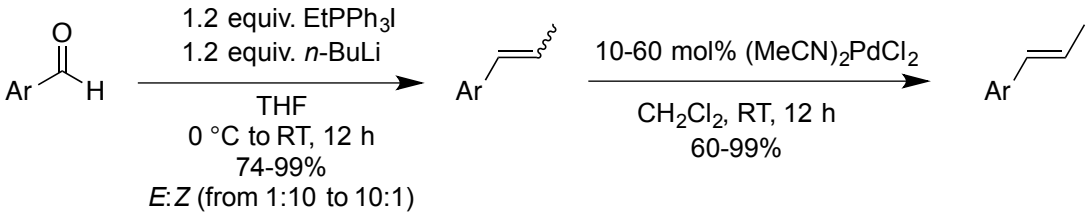
Alkenes **7**, **8**, **9**, **10**, **11**, **12**, **13** and **15** were previously synthesized in our lab and complete experimental data, including fully characterization have already been reported.[1]

A solution of triphenylphosphonium halide (1.2 equiv.) in dry solvent (5.0 mL/mmol of THF or Et_2O) was placed in a flame-dried round-bottomed flask. The solution was cooled to 0 °C, and the base (1.1 equiv. of *t*-BuOK or 1.2 equiv. of *n*-BuLi or 1.2 equiv. of NaH) was added in one portion. After stirring at 0 °C for 30 min, the aldehyde (1.0 equiv.) was added. The reaction mixture was gradually warmed to room temperature. After 12 h, the reaction was quenched by slow addition of saturated NH_4Cl. The phases were separated, and the aqueous phase was extracted twice with Et_2O. The combined organic layers were washed with brine and dried over Na_2SO_4. The solvent was

evaporated under reduced pressure to give the corresponding styrene, that was purified by chromatography on silica gel using the appropriate mixture of eluents.

For those examples where the styrene was isolated as a *Z*:*E* mixture of isomers, isomerization of *Z* isomer to *E* was performed as follows.

To a solution of the *Z:E* mixture of styrene in CH_2Cl_2 (2.0 mL/mmol) bis(acetonitrile)palladium (II) chloride (10 – 60 mol%) was added at room temperature. The reaction was monitored by ^1H NMR until completion, diluted with diethyl ether and filtered through a short pad of Florisil™, eluting with diethyl ether. The solvent was evaporated under reduced pressure to give the corresponding *E*-styrene, that was purified by chromatography on silica gel using the appropriate mixture of eluents.[2]



2. Cyclic voltammetry details

Voltammetry is a dynamic technique sensitive to both the interfacial electron transfer kinetics and also the prevailing mass-transport to and from the electrochemical interface. Consequently, for a diffusional redox process determining the number of electrons transferred during a voltammetric process requires knowledge of the diffusion coefficient of the reactant. The peak-height (I_p) of the voltammetric response of an irreversible multi-electron process at a macro-electrode is parametrically given by the irreversible form of the Randles-Sevcik;[3]

$$I_p = 2.99x10^5 n(n' + \alpha_{rds})^{0.5} D^{0.5} A C \nu^{0.5}$$

where n is the total number of electrons transferred, n' is the number of electrons transferred prior to the rate determining step, α_{rds} is the transfer coefficient[4] associated with the rate determining electron transfer step, D is the diffusion coefficient, A is the geometric area of the electrode, C is the solution phase concentration of the redox species and ν is the voltammetric scan rate. The term $(n' + \alpha_{rds})$ can be experimentally measured via a Tafel plot (lnlil vs E). Consequently, experimental use of this equation will yield a value for the product $nD^{0.5}$.

One route by which the individual values of n and D can be resolved is by changing the mass-transport regime. In this work the steady-state response at an ultramicroelectrode is used to enable n and D to be resolved. At high overpotentials the magnitude of faradaic current for the oxidation or

reduction of a solution phase species is insensitive to the kinetics of the electron transfer process and the steady-state response is given by:[3]

$$I_{ss} = 4nFDCr$$

where n is the total number of electrons transferred, F is the Faraday constant (96485 C mol^{-1}), D is the diffusion coefficient, C is the solution phase concentration of the redox species and r is the radius of the microdisc electrode. Hence, experimental determination of the steady-state Faradaic current yields a value for the product nD. Due to the differing sensitives to the magnitude of the diffusion coefficient, and by assumption that the value of n is the same under both mass-transport regimes (and is an integer value representing the stoichiometric number of electrons transferred), then the values of n and D are experimentally accessible.

In the following the voltammetric experimental details for the oxidation of *trans*-anethole in both HFIP and ACN at a macro- and micro-disc electrode is reported enabling from in accordance with the above discussion for n and D to be determined. The voltammetry for the oxidation of *trans*-anethole in ACN and HFIP in the presence of ferrocene is also shown so that the *trans*-anethole oxidative peak potential may be measured.

2.1. *trans*-Anethole Oxidation in ACN

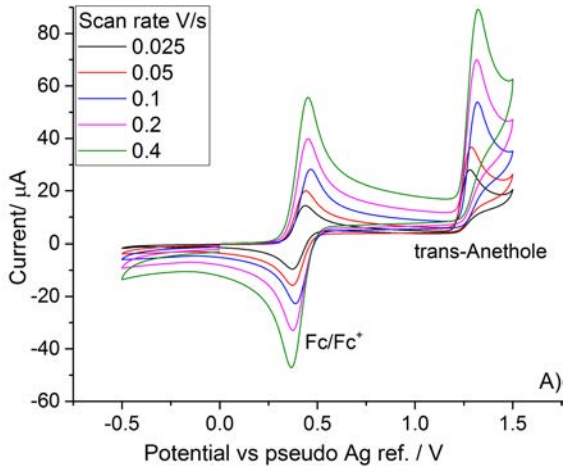


Figure 1: Oxidation of *trans*-anethole 1.0 mM, and Ferrocene 1.0 mM, 0.1 M Bu_4NPF_6 in ACN variable scan rate 0.025-0.4 V/s glassy C electrode radius = 1.5 mm.

The oxidation of *trans*-anethole (1 mM) was studied in the presence of 1 mM ferrocene in ACN as a function of scan rate. From the literature the oxidation reaction is known to proceed via a one electron oxidation of the *trans*-anethole, where the species has a reported diffusion coefficient of $2x10^{-9}$ m^2 s^{-1}.[5]

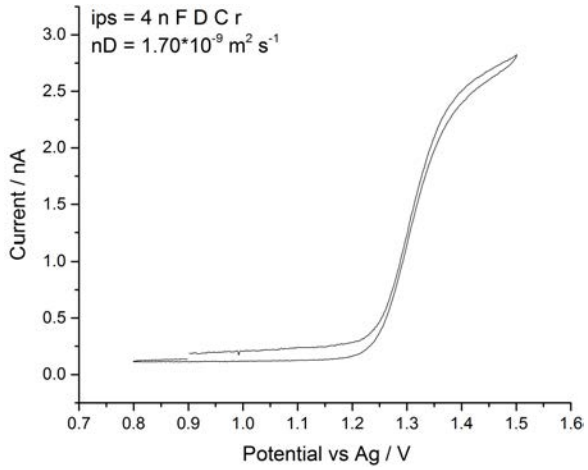


Figure 2: The oxidation of 1 mM *trans*-anethole in ACN at a carbon fibre microelectrode.

From Tafel analysis the first electron oxidation of the *trans*-anethole was found to be near reversible with the transfer coefficient measured as ~1. Given the reported diffusion coefficient of *trans*-anethole to be $2x10^{-9}$ m^2 s^{-1} the steady-state response confirms that the oxidative processes involves the transfer of one-electron.

2.2. *trans*-Anethole Oxidation in HFIP

Figure 1 A) of the main text depicts the voltammetric response of *trans*-anethole at a macro glassy carbon electrode. The figure below depicts the variation of the peak height as a function of scan rate. Tafel analysis yielded a transfer coefficient for the oxidation of *trans*-anethole on HFIP to be 0.723, indicating that the electron transfer is likely quasi-reversible.

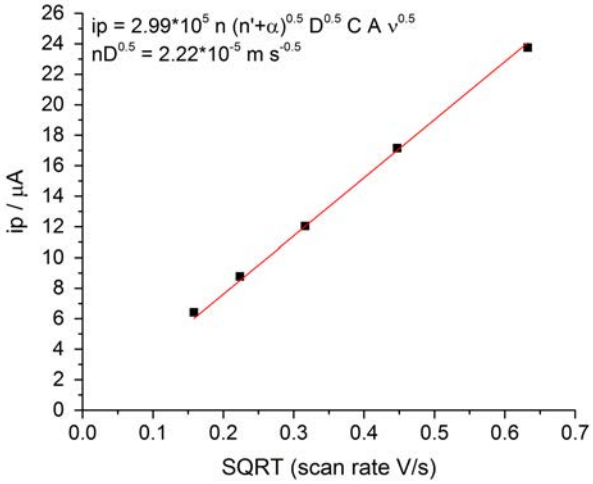


Figure 3: Variation of the measured peak height as a function of scan rate for the oxidation of *trans*-anethole 1.0 mM, 0.1 M Bu_4NPF_6 in HFIP at a glassy C electrode radius = 1.5 mm. Line of best fit shown in red and the analysis of the gradient is undertaken using the irreversible form of the Randles-Ševčík equation.

The oxidation of the *trans*-anethole was also recorded at a carbon fibre microelectrode from comparison of the currents measured under the differing mass-transport regimes it was concluded that the oxidative process involves the transfer of one electron.

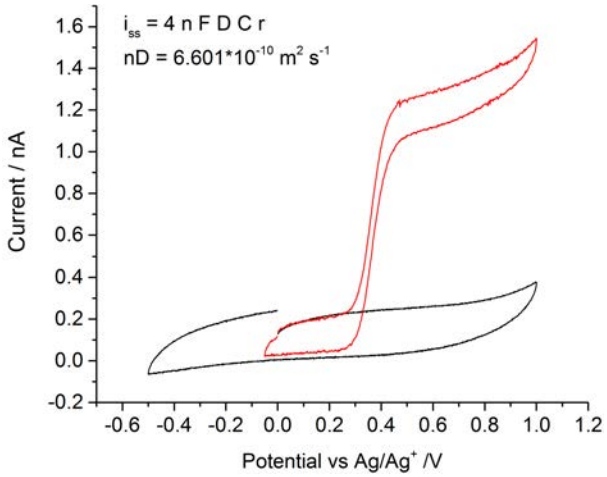


Figure 4: Oxidation of *trans*-anethole 1.2 mM, 0.1 M Bu_4NPF_6 in HFIP at 0.025 V/s using a micro carbon electrode radius = 3.5 µm.

2.3. PIDA reduction in ACN

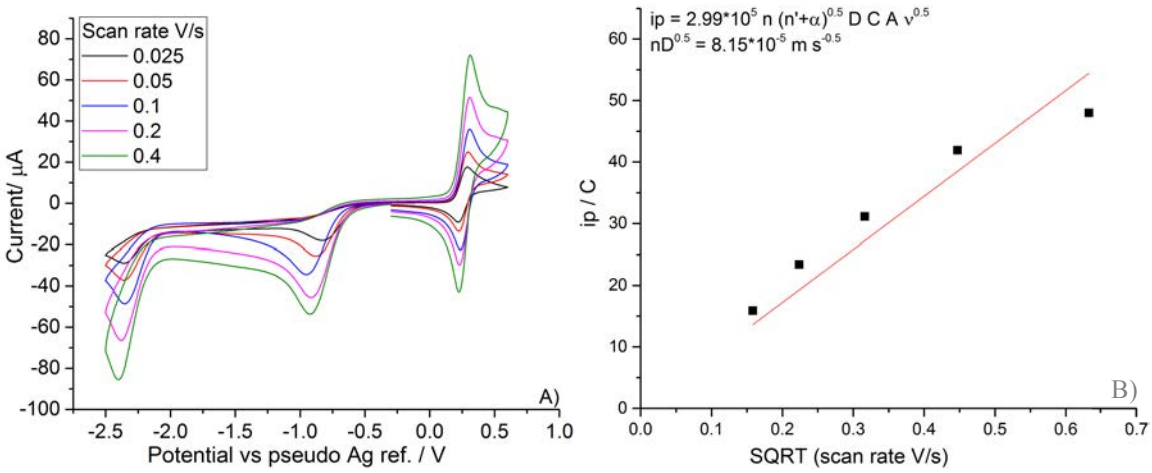


Figure 5: A) Reduction of PIDA 1.0 mM, and Ferrocene 1.0 mM, 0.1 M Bu_4NPF_6 in ACN variable scan rate 0.025-0.4 V/s at a glassy C electrode radius = 1.5 mm. B) Variation of the measured peak height as a function of scan rate and the analysis of the gradient using the irreversible form of the Randles-Ševčík

From Tafel analysis the transfer coefficient for the reduction was determined to be 0.25.

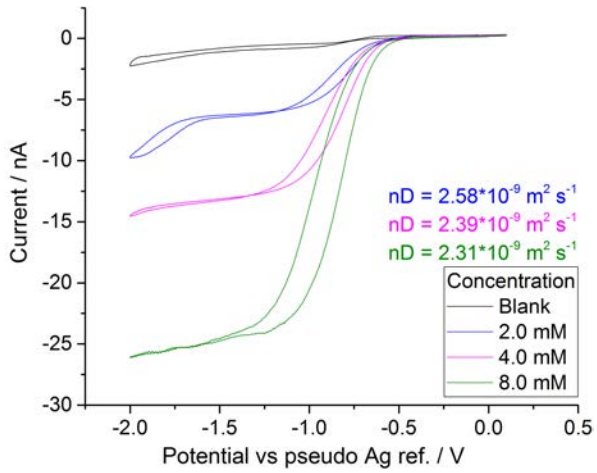


Figure 6: Reduction of PIDA 1 mM, 0.1 M Bu_4NPF_6 in ACN at 0.025 V/s using a micro carbon electrode radius = 3.5 µm

By comparison of the results from the macro and micro electrode data it was determined that over the voltammetric timescale the total number of electrons transferred in the first reduction wave is likely to be equal to three.

2.4. PIDA reduction in HFIP

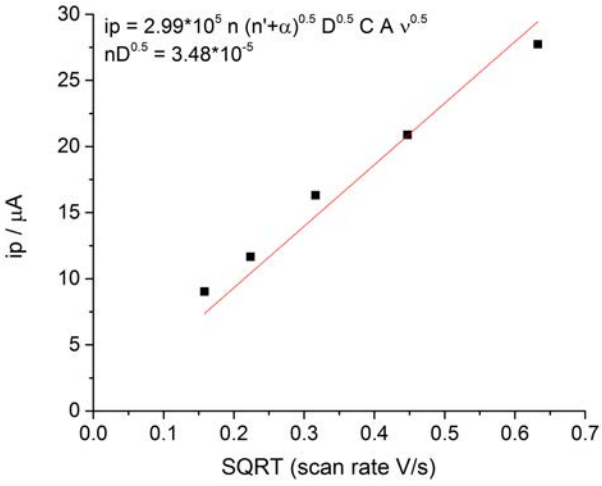


Figure 7: Variation of the measured peak height as a function of scan rate for the reduction of PIDA 1.0 mM, 0.1 M Bu_4NPF_6 in HFIP at a glassy C electrode radius = 1.5 mm. Line of best fit shown in red and the analysis of the gradient is undertaken using the irreversible form of the Randles-Ševčík equation.

Tafel analysis indicted the transfer coefficient to be 0.4.

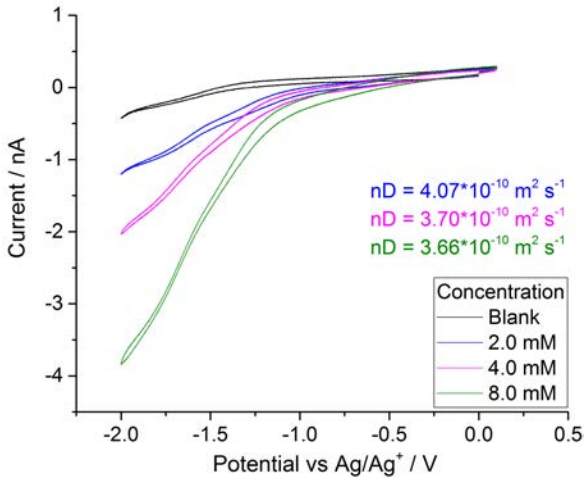


Figure 8: Reduction of PIDA 1 mM, 0.1 M Bu_4NPF_6 in HFIP at 0.025 V/s using a micro carbon electrode radius = 3.5 µm

Although the reduction wave for PIDA in HFIP recoded at the microelectrode does not show a clear steady-state region the resulting currents are not inconsistent with the conclusion that a total of three electrons are being transferred to the PIDA over the voltammetric timescale.

2.5. Ferrocene oxidation measured against Ag/Ag+ reference

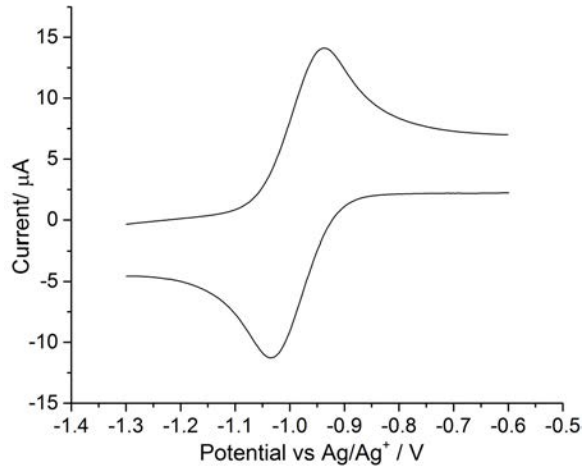


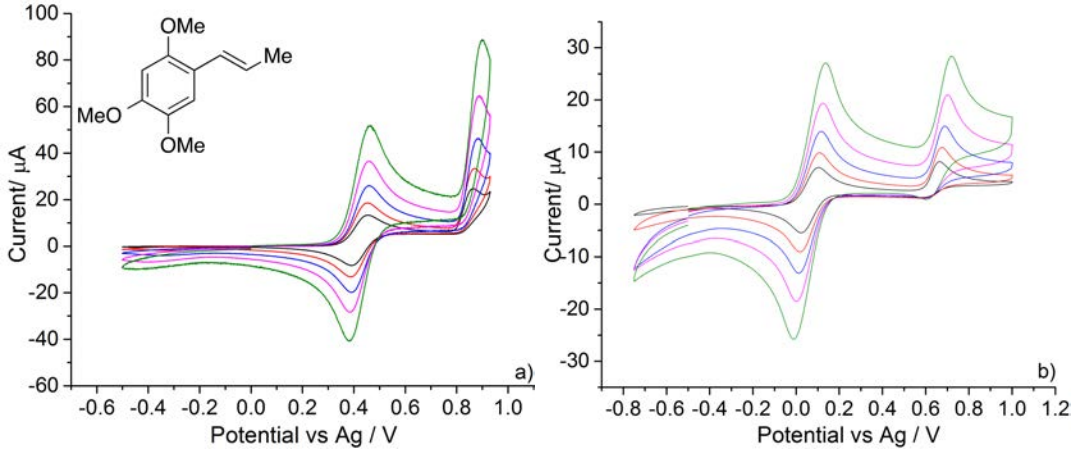
Figure 9: The redox response of 1 mM ferrocene in a 0.1 M Bu_4NPF_6 HFIP at a glassy carbon macro-electrode (radius = 1.5 mm) solution as measured against the Ag/Ag+ reference electrode at a scan rate of 0.1 V s^{-1}

2.6. Voltammetric characterisation of the alkenes in both ACN and HFIP

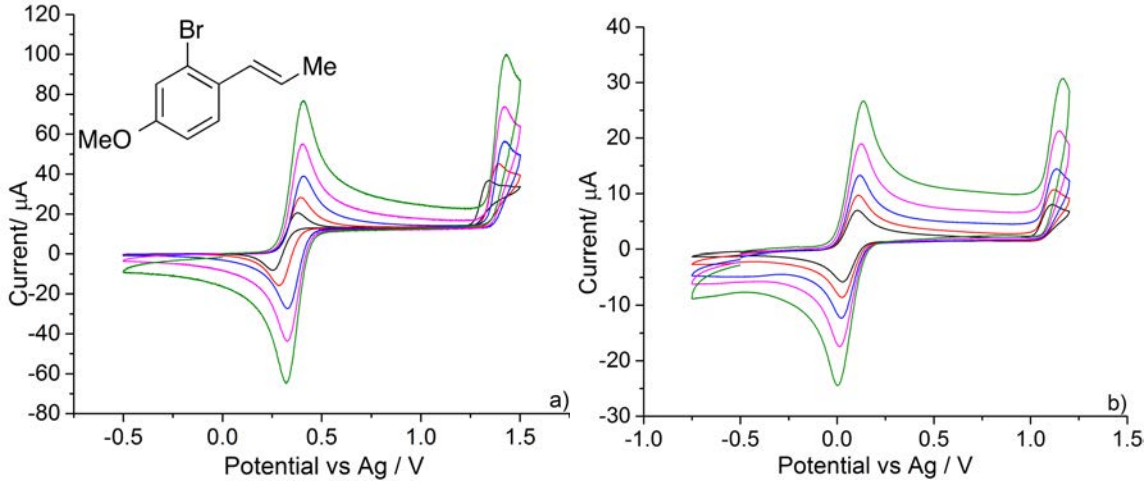
All voltamemtric results have been recorded at a glassy carbon macroelectrode (radius = 1.5mm). Scan rates used range from 0.025-0.4 V s^{-1}. Electrolyte 0.1M Bu_4NPF_6.

a) Measured in ACN b) Measured in HFIP

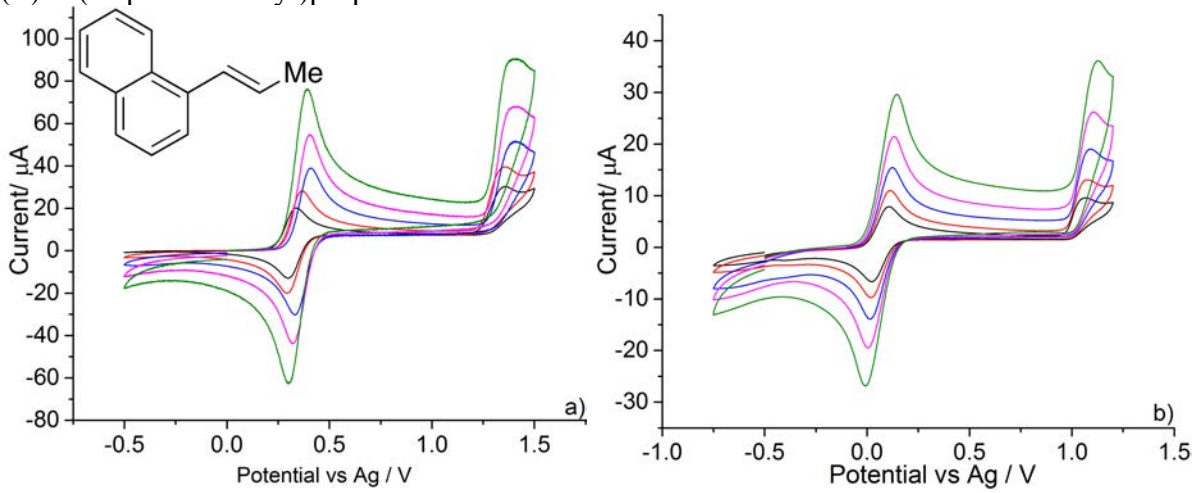
E-Asarone



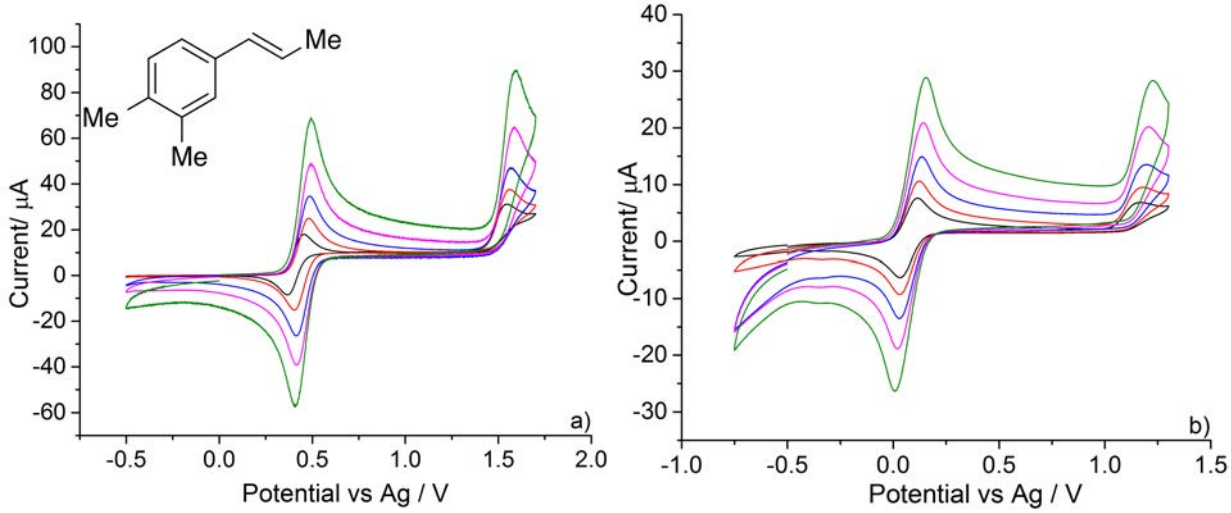
(*E*)-1-(2-Bromo-4-methoxyphenyl)prop-1-ene



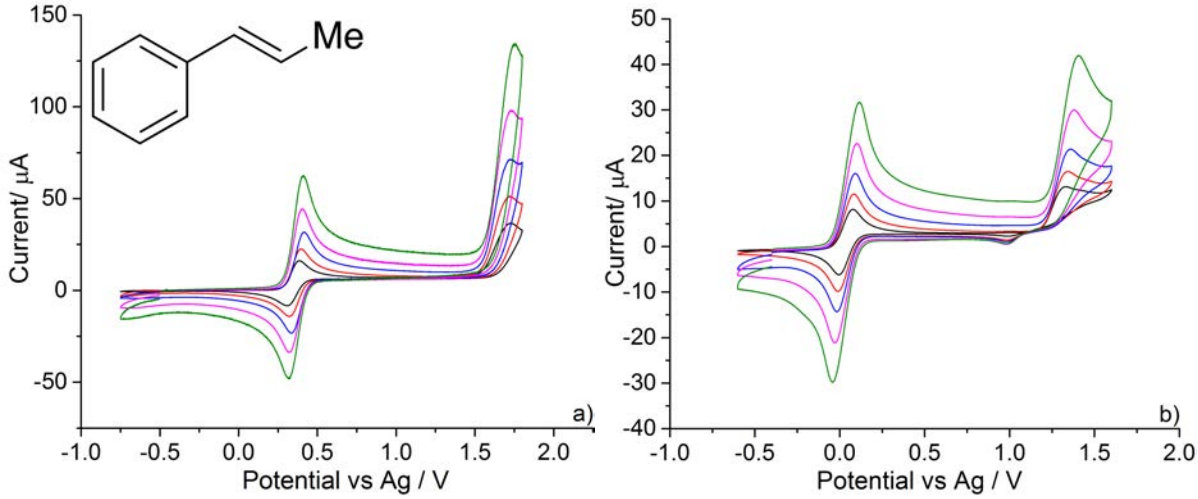
(*E*)-1-(Naphthalen-1-yl)prop-1-ene



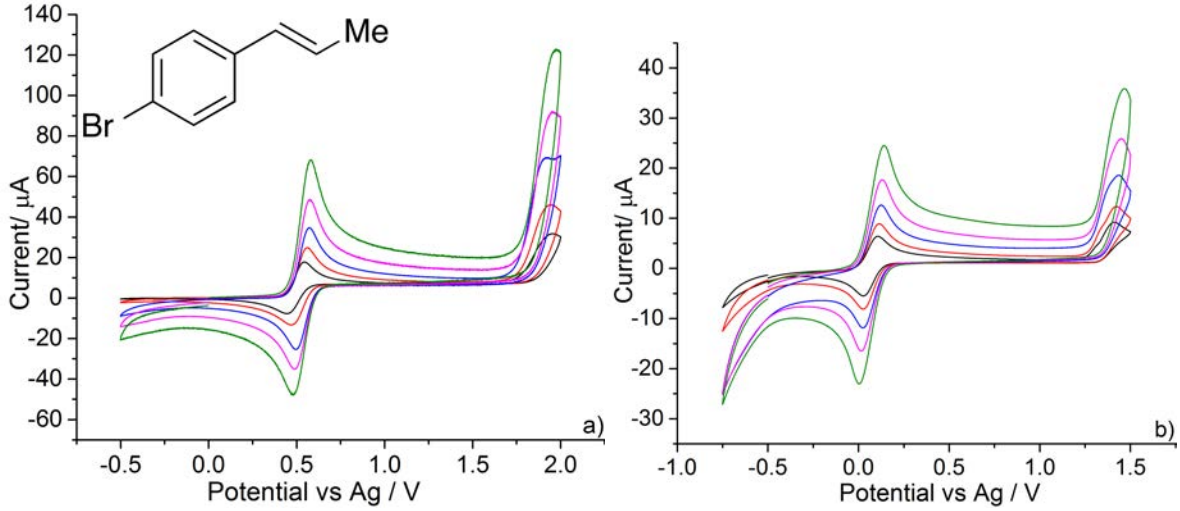
(*E*)-1-(3,4-Dimethylphenyl)prop-1-ene



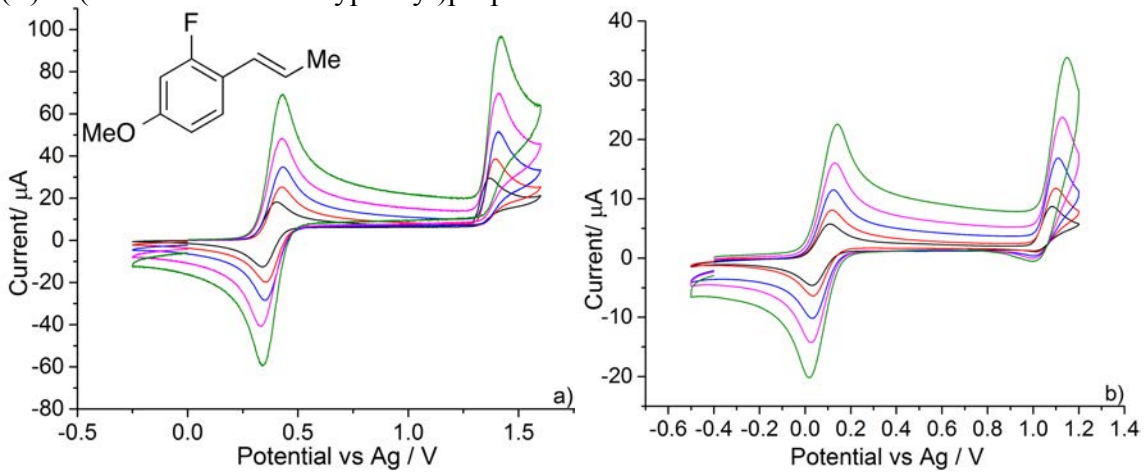
trans-β-Methylstyrene



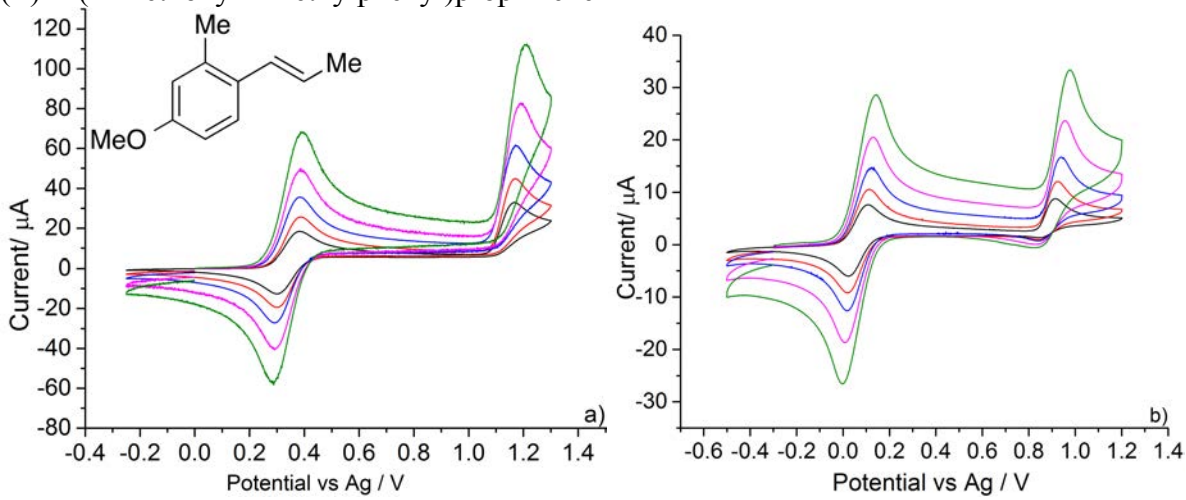
(*E*)-1-(4-Bromophenyl)prop-1-ene



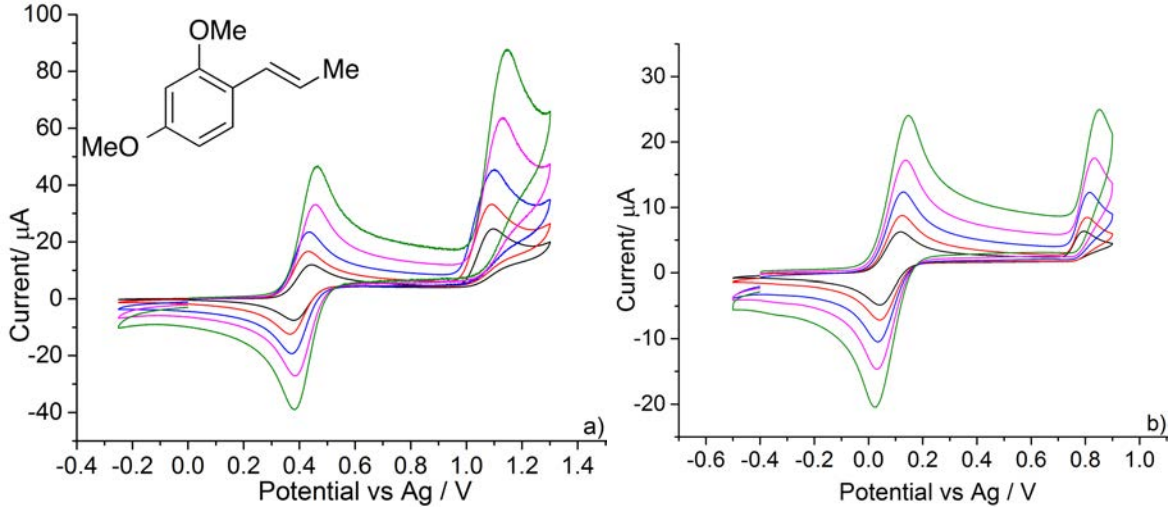
(*E*)-1-(2-Fluoro-4-methoxyphenyl)prop-1-ene



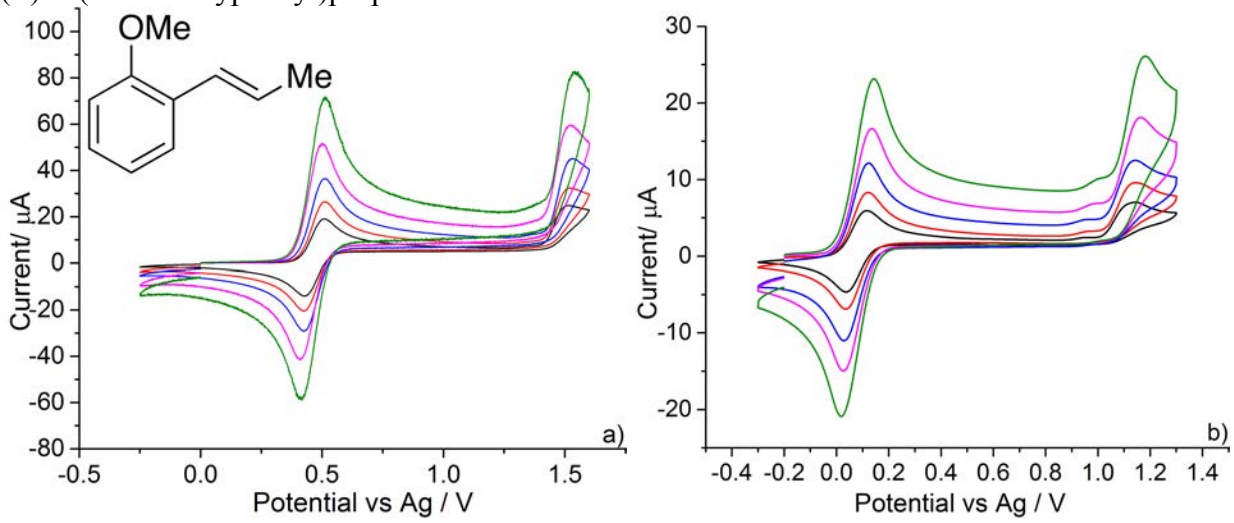
(*E*)-1-(4-Methoxy-2-methylphenyl)prop-1-ene



(*E*)-1-(2,4-Dimethoxyphenyl)prop-1-ene



(*E*)-1-(2-Methoxyphenyl)prop-1-ene



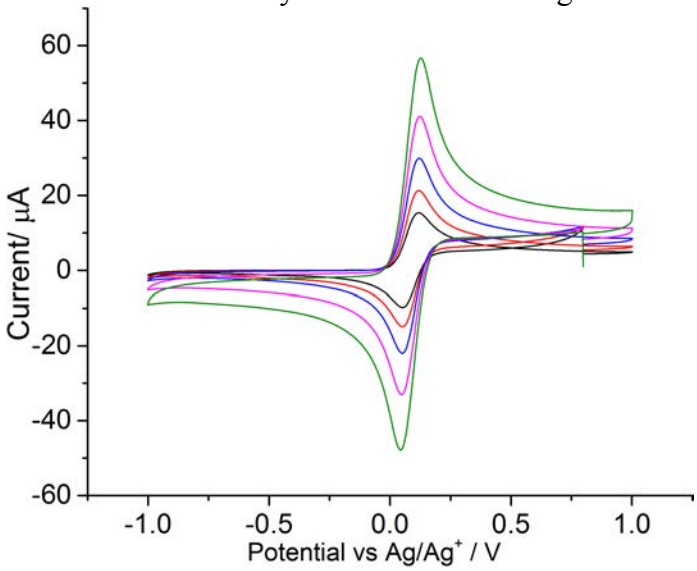
2.7. Voltammetric characterisation of iodine (III) reagents PIFA and HTIB.

All voltammetric results have been recorded at a glassy carbon macroelectrode (radius = 1.5mm). Scan rates used range from 0.025-0.4 V s-1. Electrolyte 0.1M Bu_4NPF_6.

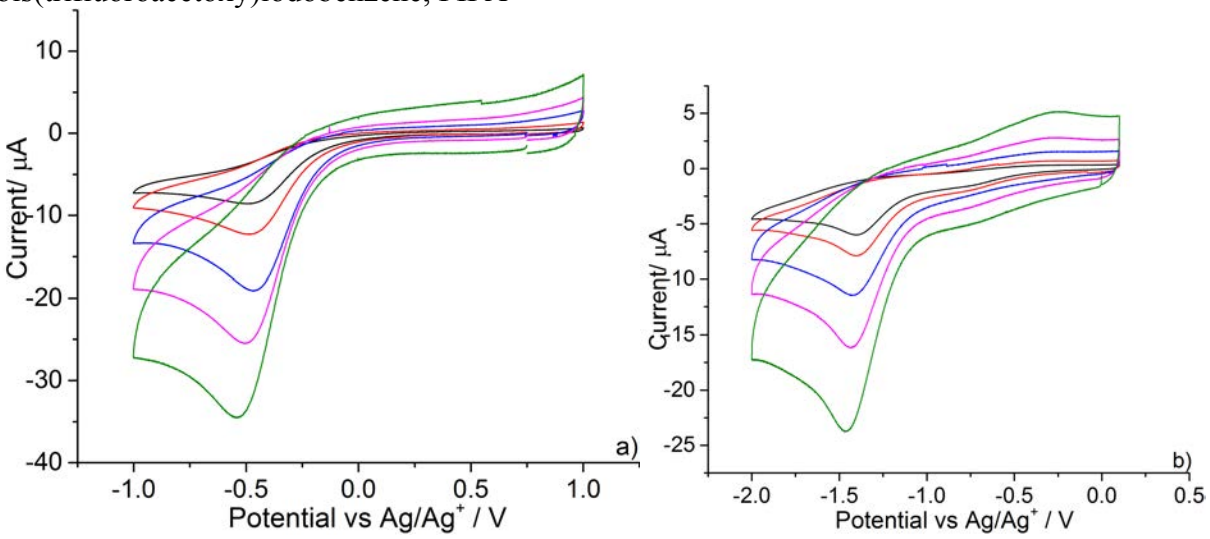
a) Measured in ACN b) Measured in HFIP.

Due to the reactivity of PIFA and HTIB in ACN, the voltammograms of these species had to be measured using an Ag/Ag+ reference electrode. The potential of the Fc/Fc+ redox couple againset the Ag/Ag+ reference electrode was found to be +0.086 V, the corresponding voltammetric measurement showing this is depicted below. Note as shown above in the SI section 2.5, the Fc/Fc^+ redox couple occurs at -0.988 V vs Ag/Ag^+ in HFIP.

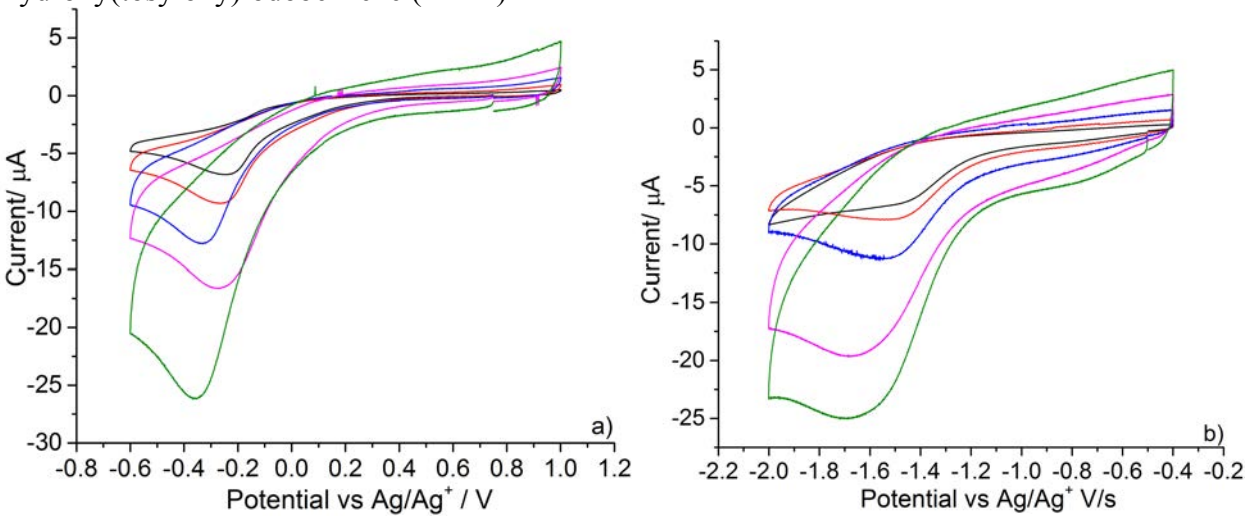
Ferrocene voltammetry in ACN measured against an Ag/Ag+ reference electrode.



bis(trifluoroacetoxy)iodobenzene, PIFA



Koser's Reagent
Hydroxy(tosyloxy)iodobenzene (HTIB)

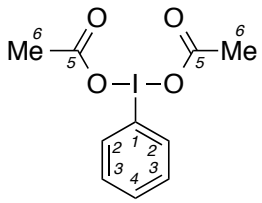


3. Mass Spectrometry experimental details

High resolution mass spectra are given to four decimal places under conditions of electrospray ionization (ESI). The experiments were carried on using acetonitrile as solvent because in this solvent any side reaction is known to be slower to avoid any decomposition of the sample. In addition, acetonitrile as a non-nucleophilic molecule does not react by nucleophilic attack on hypervalent iodines. Analyses were performed using a Thermo Exactive mass spectrometer equipped with Waters Acquity liquid chromatography system. Instrument control and data processing were performed using Thermo Xcalibur Software. The system was calibrated on the day of the analysis and its mass accuracy with external calibration (as used for these experiments) is better than 5ppm for 24 hours following calibration. The mass spec was operated using the heated electrospray (HESI-II) probe and resolution was set to 50,000. Electrospray source conditions were

adjusted to maximise sensitivity. Acetonitrile was used to transport samples to the mass spectrometer at a flow rate of 0.2 mL/min.

3.1. HRMS of PIDA (2)



2

HRMS (ESI): The main peaks observed correspond to the following ionized species:

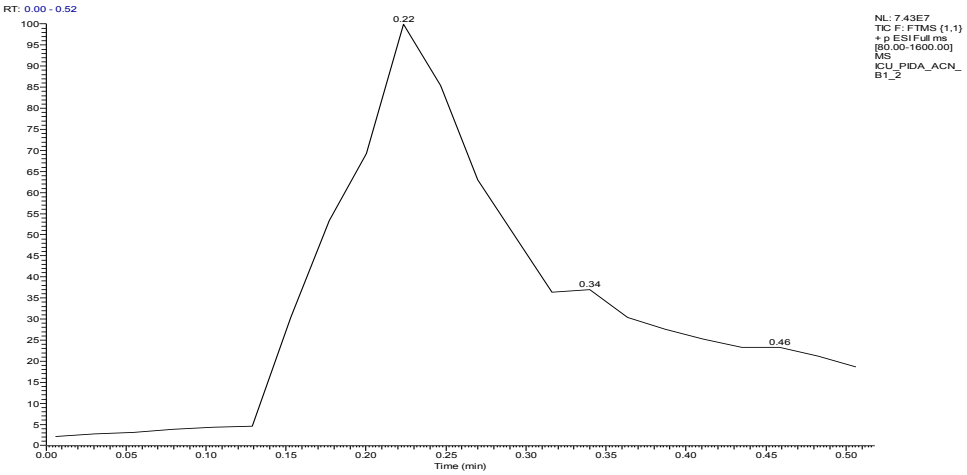
$[PhI(OAc)_2+Na]^+$ calculated for $C_{10}H_{11}INaO_4$ requires *m*/*z* 344.9600, found *m*/*z* 344.9588.

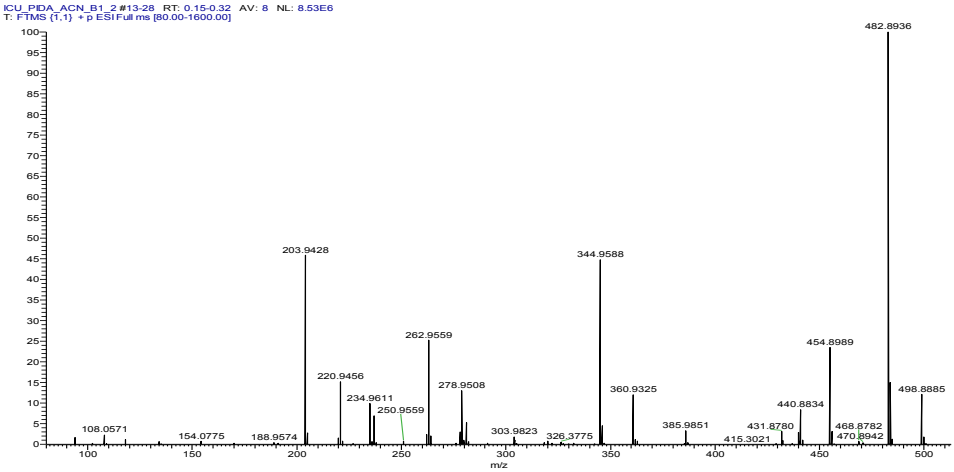
$[PhI(OAc)_2+K]^+$ calculated for $C_{10}H_{11}IKO_4$ requires *m*/*z* 360.9339, found *m*/*z* 360.9325.

$[PhIOAc]^+$ calculated for $C_8H_8IO_2$ requires *m*/*z* 262.9554, found *m*/*z* 262.9559.

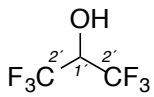
$[PhI]^{\cdot+}$ calculated for C_6H_5I requires *m*/*z* 203.9430, found *m*/*z* 203.9428.

$[Ph(OAc)OIPh]^+$ calculated for $C_{14}H_{13}I_2O_3$ requires *m*/*z* 482.8954, found *m*/*z* 482.8936.





3.2. HRMS of HFIP (3)

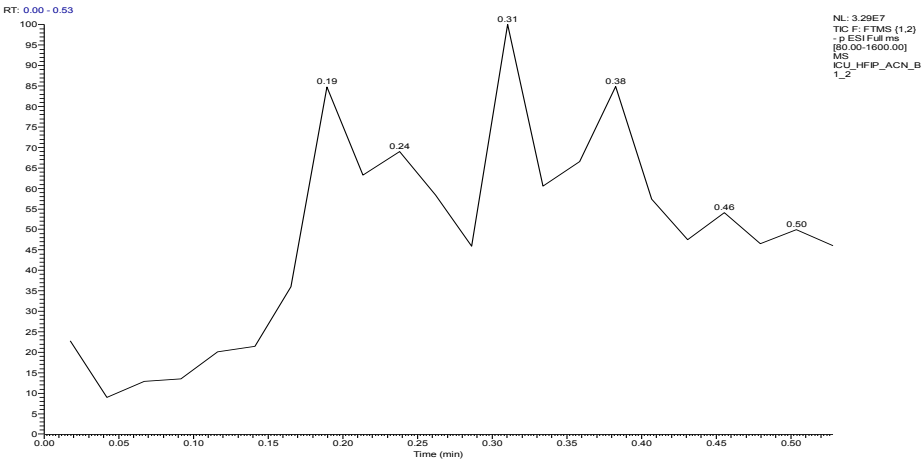


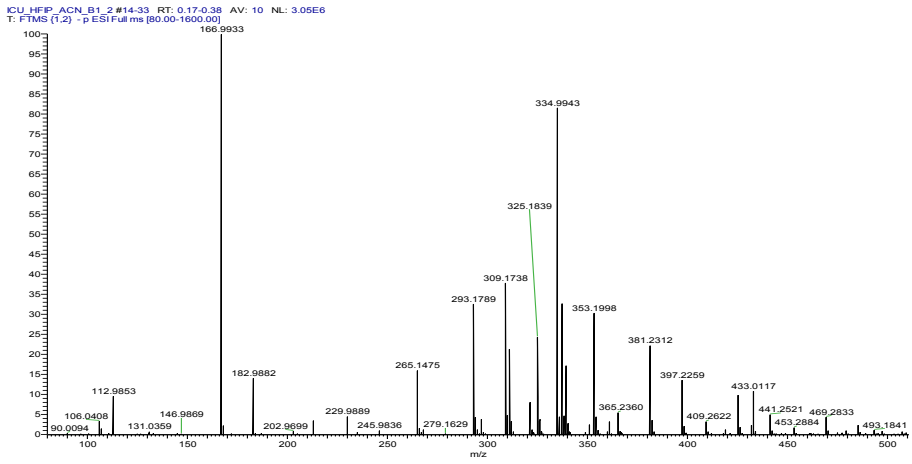
3

HRMS (ESI): The main peaks correspond to the following ionized species:

$[(CF_3)_2CHO]^-$ calculated for C_3HF_6O requires *m*/*z* 166.9932, found *m*/*z* 166.9934.

$[2M - H]^-$ calculated for $C_6H_3F_{12}O_2$ requires *m*/*z* 334.9941, found *m*/*z* 334.9943.





3.3. HRMS of a 1:1 mixture of HFIP:PIDA (5)

HRMS (ESI): The main peaks observed are the same as the obtained above for PIDA (**2**) corresponding to the following ionized species, derived from the ionization of PIDA (**2**):

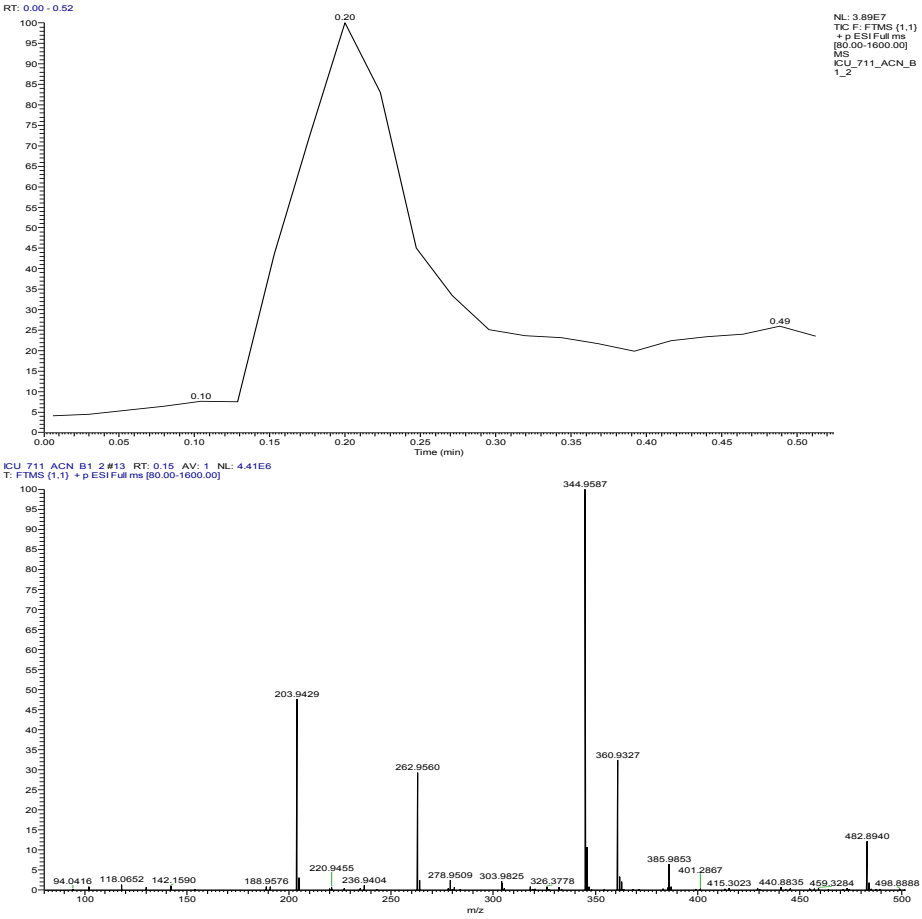
$[PhI(OAc)_2+Na]^+$ calculated for $C_{10}H_{11}INaO_4$ requires *m*/*z* 344.9600, found *m*/*z* 344.9587.

$[PhI(OAc)_2+K]^+$ calculated for $C_{10}H_{11}IKO_4$ requires *m*/*z* 360.9339, found *m*/*z* 360.9327.

$[PhIOAc]^+$ calculated for $C_8H_8IO_2$ requires *m*/*z* 262.9554, found *m*/*z* 262.9560.

$[PhI]^{\cdot+}$ calculated for C_6H_5I requires *m*/*z* 203.9430, found *m*/*z* 203.9429.

$[Ph(OAc)OIPh]^+$ calculated for $C_{14}H_{13}I_2O_3$ requires *m*/*z* 482.8954, found *m*/*z* 482.8940.



4. NMR experimental details

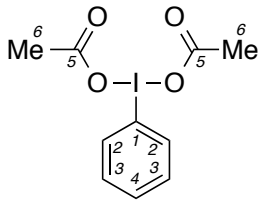
All the NMR experiments were recorded on a Bruker AVIIIHD 400 nanobay or Bruker AVII 500 spectrometer in $CDCl_3$, and referenced to residual solvent peaks. All spectra were acquired in a 5 mm inverse probehead at 298 K in 5 mm tubes. Chemical shifts are quoted in ppm (parts per million) to the nearest 0.01 ppm with signal splitting recorded as singlet (s), doublet (d), triplet (t), quartet (q), quintet (quin), sextet (sex), septet (sept), multiplet (m) and broad singlet (br. s). Coupling constants, *J*, are measured in Hz to the nearest 0.1 Hz.

2D NOESY spectra were collected using the standard Bruker pulse programs *noesyph* or *noesygpph* (90-t_1-90-τ_m-90-Acq, without or with a purging bipolar gradient pulse pair (G_1-180-[-]G_1) at the midpoint of the mixing period) with mixing times of 800 ms at the temperatures and in the solvents stated. For each data set, 8 or 16 transients were acquired for each of 256 increments with 2K data points per spectrum, using recovery times of 2 s. Data were processed typically as 1K x 1K data points using shifted squared-sinebell apodisation windows (WDW=QSINE, SSB=2).

DOSY NMR measurements were performed using a Bruker AVII-500 equipped with a TFI probehead at 298°K with constant temperature control (air flow 400 l h^{-1}) using the 2D sequence

for diffusion measurement using double stimulated echo for convection compensation and longitudinal eddy current delay, using bipolar gradient pulses for diffusion, and using three spoil gradients (Bruker terminology: dstebpgp35) pulse sequence. Diffusion data were collected using 32K data points on well mixed homogeneous samples in de-acidified $CDCl_3$ containing TMS as a suitable internal reference. Experiments were performed in two stages: 1) initially 1D-edited DOSY experiments were used to optimize the diffusion period Δ for each sample (Δ=100 ms) and 2) the 2D dstebpgp35 sequence was then used, based on the optimized Δ from the previous procedure and with δ=4 ms, with gradient amplitudes ranging from 2 to 85% using 16 increments (difflist). Diffusion constants were obtained directly employing the T1/T2 module in TOPSPIN 3.2 using the variable gradient function and plots were generated using the eddosy module.

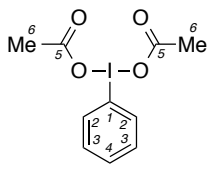
4.1. ^{1}H and ^{13}C NMR of PIDA



2

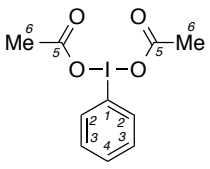
Data for **2**: **^{1}H NMR (400 MHz)** δ 8.08 (2 H, dd, *J* = 8.3 and 1.6 Hz, 2-H), 7.59 (2 H, tt, *J* = 7.4 and 1.1 Hz, 3-H), 7.49 (1 H, tt, *J* = 7.7 and 1.5 Hz, 4-H), 2.00 (6 H, s, 6-H_3). **^{13}C NMR (100 MHz)** δ 176.5 (2 C, C-5), 135.1 (2 C, C-2), 131.8 (C-4), 131.1 (2 C, C-3), 121.8 (C-1), 20.5 (2 C, C-6).

^{1}H NMR (400 MHz, $CDCl_3$)



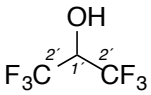
2

^{13}C NMR (100 MHz, $CDCl_3$)



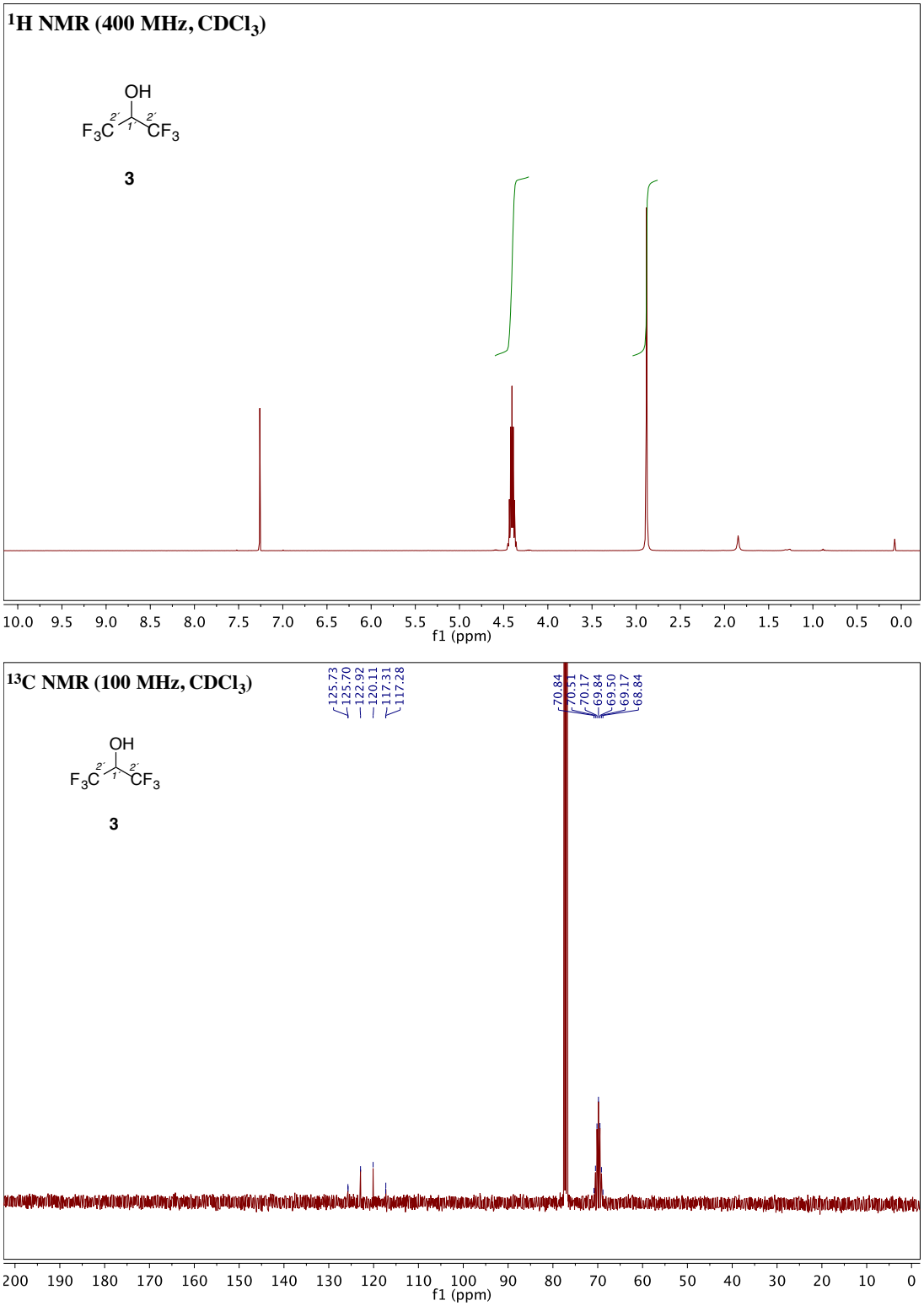
2

4.2. ^{1}H and ^{13}C NMR of HFIP

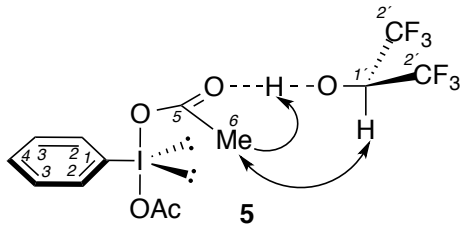


3

Data for **3**: **^{1}H NMR (400 MHz)** δ 4.41 (1 H, sept, $J_{H\text{-}F}$ = 5.9 Hz, 1′-H), 2.88 (1 H, s, OH). **^{13}C NMR (100 MHz)** δ 121.5 (2 C, q, $J_{C\text{-}F}$ = 282.6 Hz, C-2′), 69.8 (1 C, sept, $J_{C\text{-}F}$ = 33.5 Hz, C-1′).

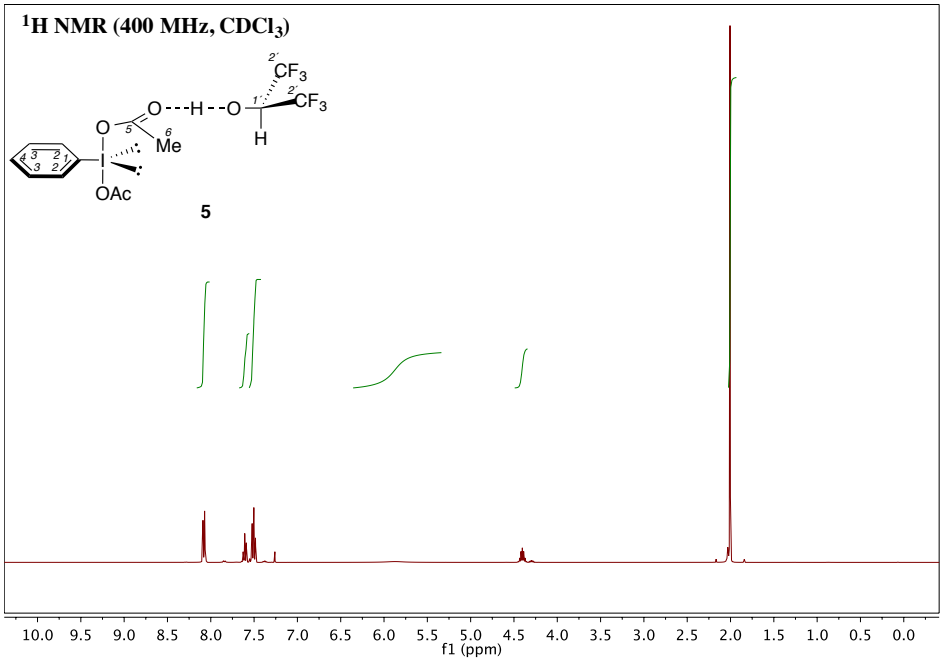


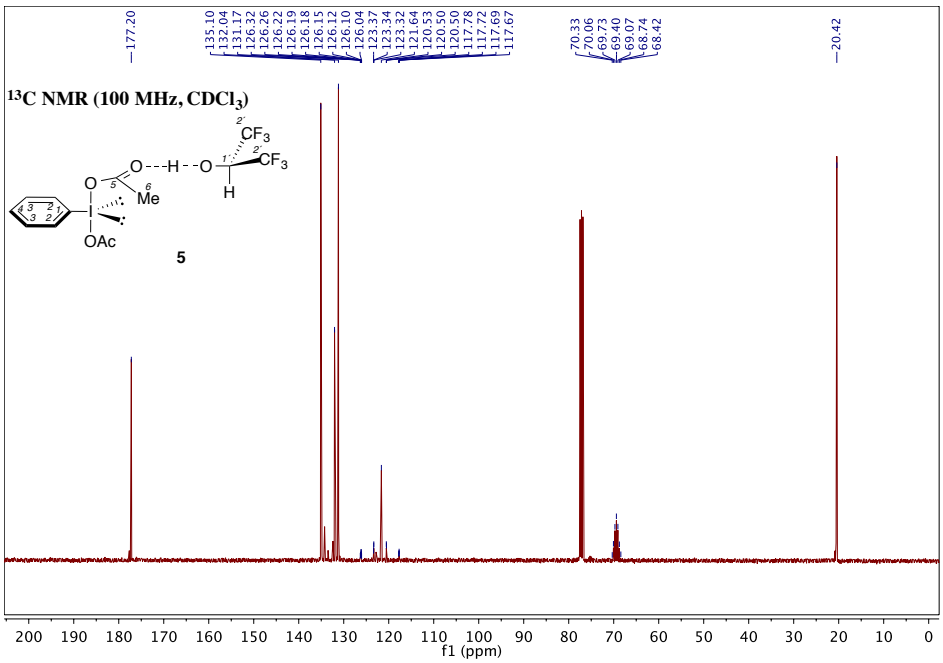
4.3. ^{1}H, ^{13}C NMR, NOESY-2D and nOe of a 1:1 mixture of HFIP:PIDA (5).



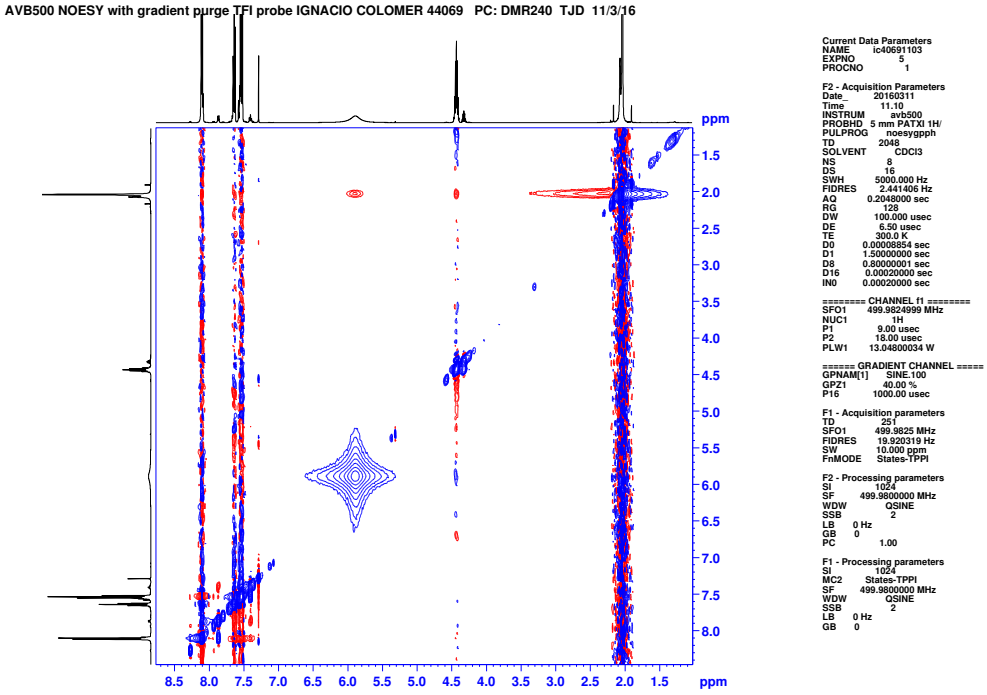
5

Data for **5**: **^{1}H NMR (400 MHz)** δ 8.08 (2 H, dd, J = 8.3 and 1.3 Hz, 2-H), 7.61 (2 H, tt, J = 7.5 and 1.1 Hz, 3-H), 7.50 (1 H, tt, J = 7.7 and 1.7 Hz, 4-H), 5.88 (1 H, br s, OH), 4.40 (1 H, sept, $J_{H\text{-}F}$ = 6.2 Hz, 1´-H), 2.01 (6 H, s, 6-H$_3$). **^{13}C NMR (100 MHz)** δ 177.2 (2 C, C-5), 135.1 (2 C, C-2), 132.0 (C-4), 131.2 (2 C, C-3), 121.9 (2 C, q, $J_{C\text{-}F}$ = 280.1 Hz, C-2´), 121.6 (C-1), 69.4 (1 C, sept, $J_{C\text{-}F}$ = 33.2 Hz, C-1´), 20.4 (2 C, C-6).

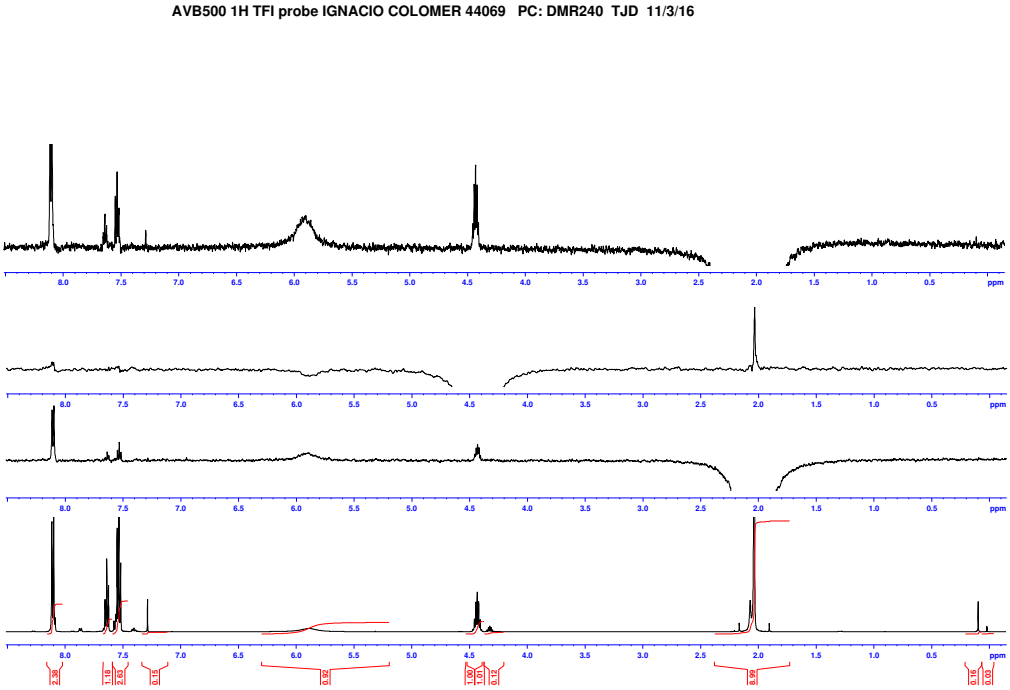




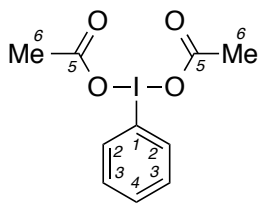
Additional support for the structure **5**, presenting an intermolecular H-bond was found upon inspection of the NOESY 2D spectra of **5**, that showed interactions between 6-H_3 and OH and between 6-H_3 and 1´-H, confirming the nature of a new bonded specie.



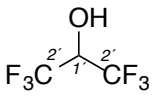
In the same manner, from the 1D nOe experiments, when irradiating the 6-H_3 nuclei we observed an nOe effect with 1´-H and with OH. In the reverse way, when irradiating 1´-H the same nOe effect is shown with 6-H_3.



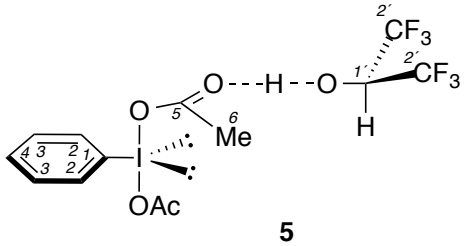
4.4. Comparison table of ^{1}H and ^{13}C NMR, for PIDA (2), HFIP (3) and a 1:1 mixture of 2:3 (5)



2



3

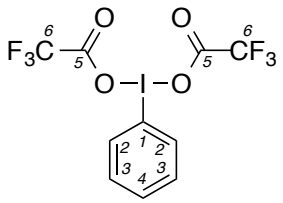


5

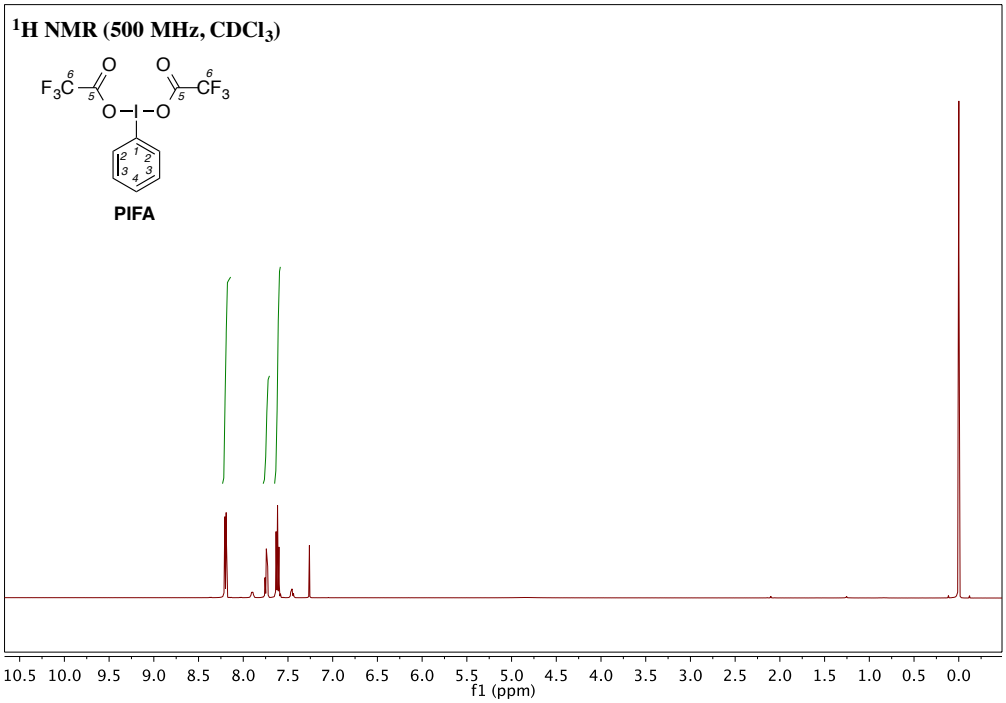
	PIDA (2)		HFIP (3)		Adduct (5)		Δδ	
	^{1}H NMR	^{13}C NMR	^{1}H NMR	^{13}C NMR	^{1}H NMR	^{13}C NMR	^{1}H NMR	^{13}C NMR
1	-	121.8	-	-	-	121.6	-	- 0.2
2	8.08 dd (8.3, 1.6)	135.1	-	-	8.08 dd (8.3, 1.3)	135.1	0.0	0.0
3	7.59 tt (7.4, 1.1)	131.1	-	-	7.61 tt (7.5, 1.1)	131.2	0.02	0.1
4	7,49 tt (7.7, 1.5)	131.8	-	-	7,50 tt (7.7, 1.7)	132.0	0.0	0.2
5	-	176.5	-	-	-	177.2	-	0.7
6	2.00 s	20.5	-	-	2.01 s	20.4	0.01	- 0.1
1´	-	-	4.41 hept (5.9)	69.8 hept (33.5)	4.40 hept (6.2)	69.4 hept (33.2)	- 0.01	- 0.4
2´	-	-	-	121.5 q (282.6)	-	121.9 q (280.1)	-	0.4
OH	-	-	2.88 s	-	5.88 br s	-	3.0	-

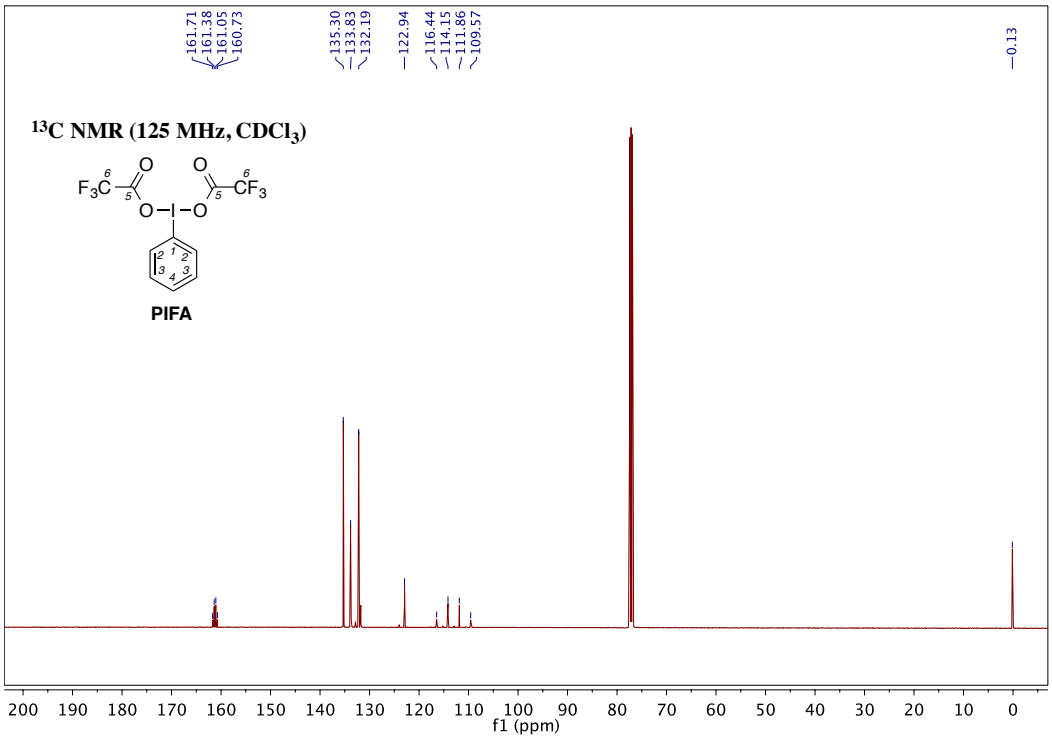
The most significant changes found in ^{1}H NMR are the down shielding shift of the O-H proton, from a frequency of 2.88 ppm to 5.88 ppm, as well as it shape, from a sharp singlet to a broad singlet. Minor changes are found in 3-H, 6-H and 1´-H with a smaller shifting of 0.01 or 0.02 ppm. Alternatively the most noteworthy changes found in ^{13}C NMR are the down shielding effect of 0.7 ppm in the carbonyl moiety (C-5) from 176.5 ppm to 177.2 ppm, as well as the 0.4 ppm shifting observed in C-1´and C-2´. Minor changes of 0.1 and 0.2 ppm are also noticed in C-3, C-4 and C-6.

4.5. ^{1}H and ^{13}C NMR of PIFA

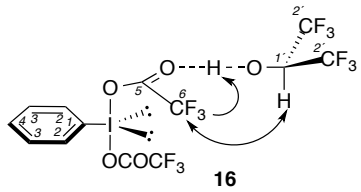


Data for **PIFA**: **^{1}H NMR (500 MHz)** δ 8.20 (2 H, d, J = 7.4 Hz, 2-H), 7.74 (1 H, t, J = 7.5 Hz, 4-H), 7.62 (2 H, t, J = 7.9 Hz, 3-H). **^{13}C NMR (125 MHz)** δ 161.2 (2 C, q, $J_{C\text{-}F}$ = 41.2 Hz, C-5), 135.3 (2 C, C-2), 133.8 (C-4), 132.2 (2 C, C-3), 122.9 (2 C, C-1), 113.0 (2C, q, $J_{C\text{-}F}$ = 288.4 Hz, C-6).



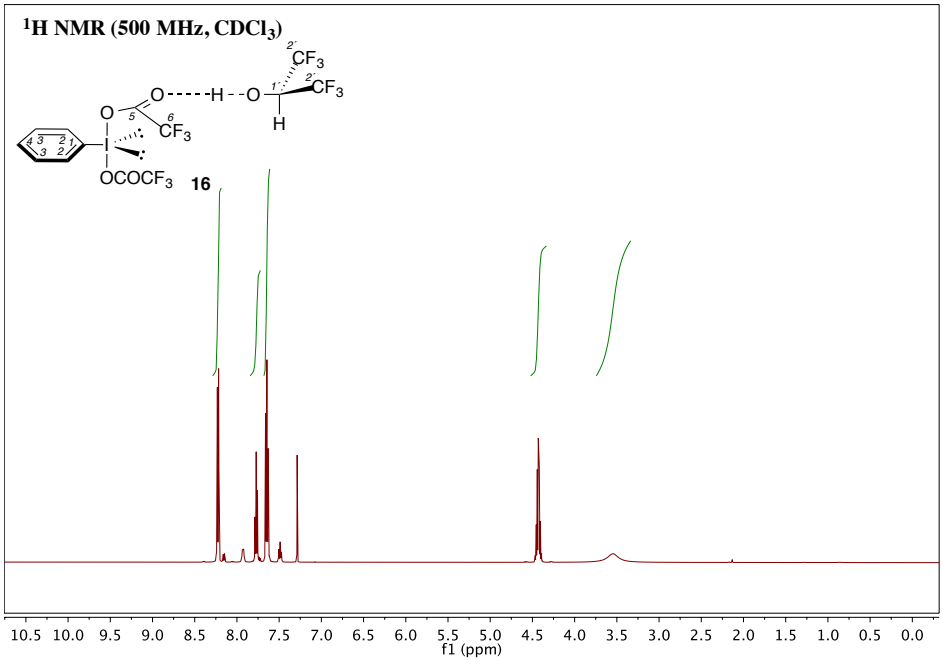


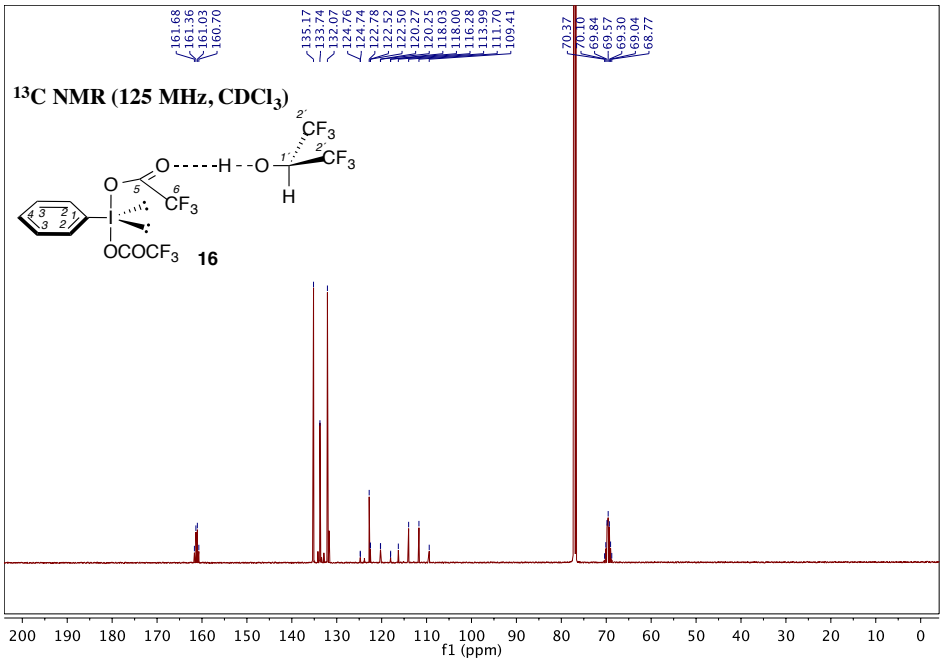
4.6. ^{1}H, ^{13}C NMR, ^{19}F and HOESY of a 1:1 mixture of HFIP:PIFA (16).



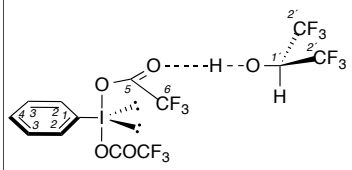
16

Data for **16**: **^{1}H NMR (500 MHz)** δ 8.22 (2 H, d, J = 7.4 Hz, 2-H), 7.77 (1 H, t, J = 7.5 Hz, 4-H), 7.65 (1 H, t, J = 7.9 Hz, 3-H), 4.43 (1 H, sept, $J_{H\text{-}F}$ = 5.9 Hz, 1′-H), 3.55 (1 H, br s, OH). **^{13}C NMR (125 MHz)** δ 161.2 (2 C, q, $J_{C\text{-}F}$ = 41.2 Hz, C-5), 135.2 (2 C, C-2), 133.7 (C-4), 132.1 (2 C, C-3), 122.8 (C-1), 121.4 (1C, qq, $J_{C\text{-}F}$ = 282.8 and 3.0 Hz, C-2′), 112.9 (2C, q, $J_{C\text{-}F}$ = 288.3 Hz, C-6), 69.6 (1 C, sept, $J_{C\text{-}F}$ = 33.6 Hz, C-1′). **^{19}F NMR (470 MHz)** δ –73.5 (CF_3, PIFA), –75.7 (CF_3, HFIP).



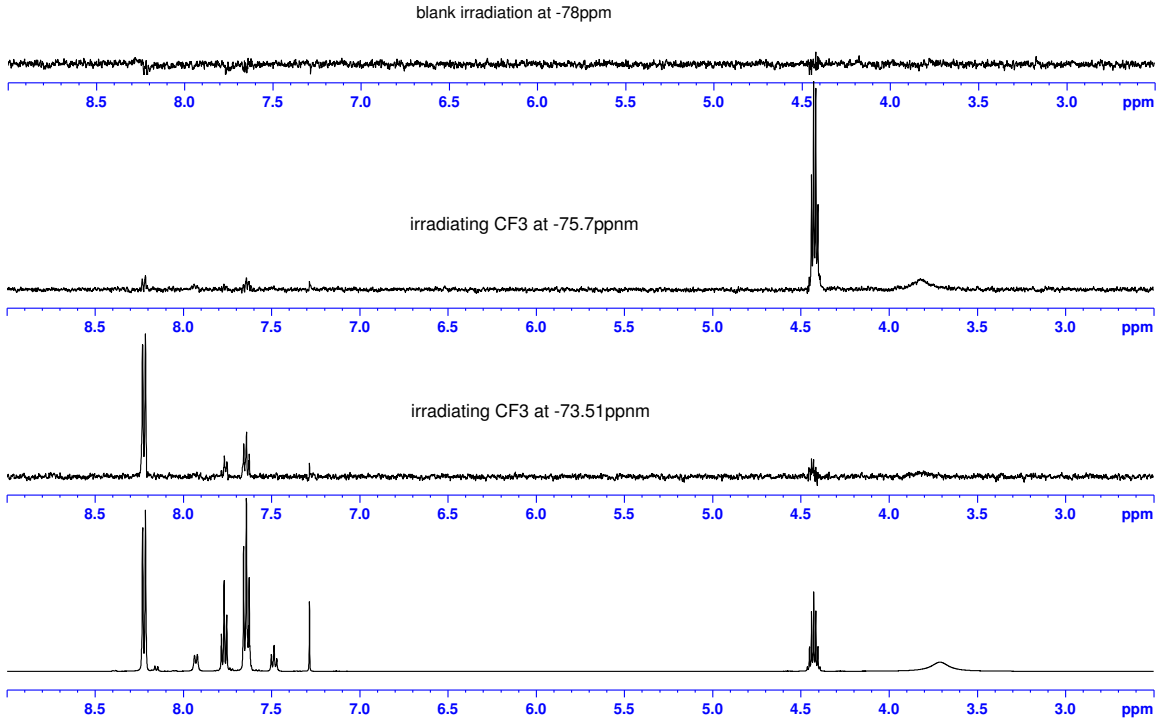


^{19}F NMR (470 MHz, $CDCl_3$)

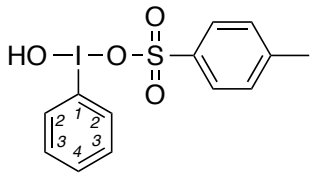


16

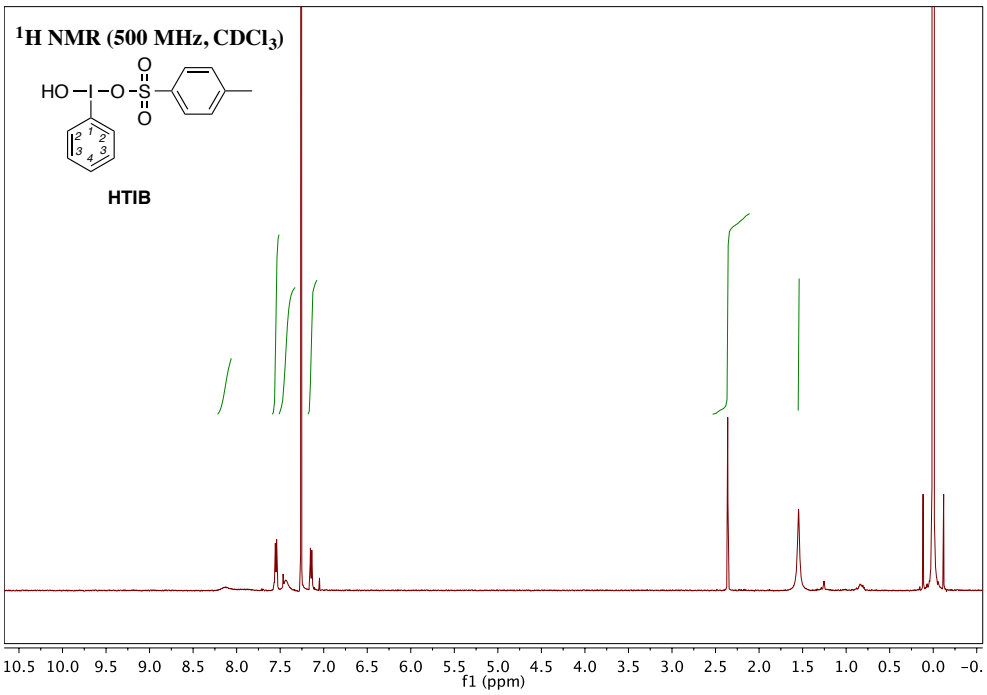
AVB500 1H TFI probe IGNACIO COLOMER 44673 PC: DMR00240 TJD 17/5/16 1-D SELECTIVE HOESY Tmix = 500msec

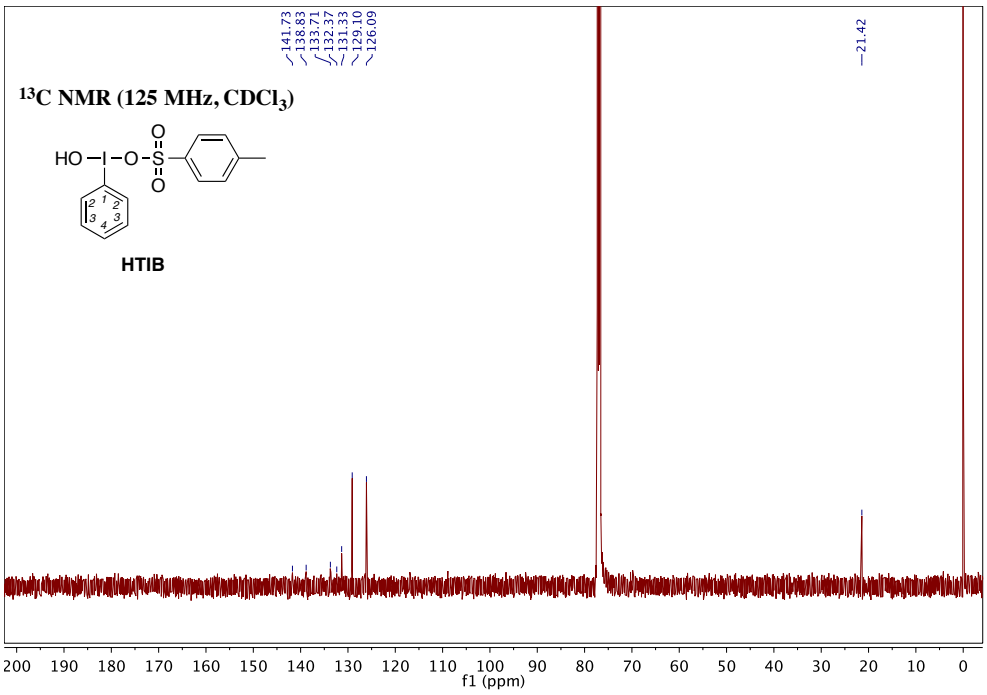


4.7. ^{1}H and ^{13}C NMR of HTIB

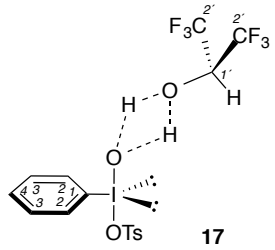


Data for **HTIB**: **^{1}H NMR (400 MHz)** δ 8.03-8.23 (2 H, m, 2-H), 7.82-7.97 (1 H, m, 4-H), 7.37-7.50 (2 H, m, 3-H), 7.55 (2 H, d, *J* = 7.5 Hz, 2 x CH Ts), 7.14 (1 H, d, *J* = 7.9 Hz, 2 x CH Ts), 2.36 (3 H, s, Me Ts), 1.55 (6 H, s, OH). **^{13}C NMR (100 MHz)** δ 141.7 (C Ts), 138.8 (C Ts), 133.7 (C-2), 132.4 (C-4), 131.3 (C-3), 129.1 (2 x CH Ts), 126.1 (2 x CH Ts), 123.5 (C-1), 21.4 (Me Ts).



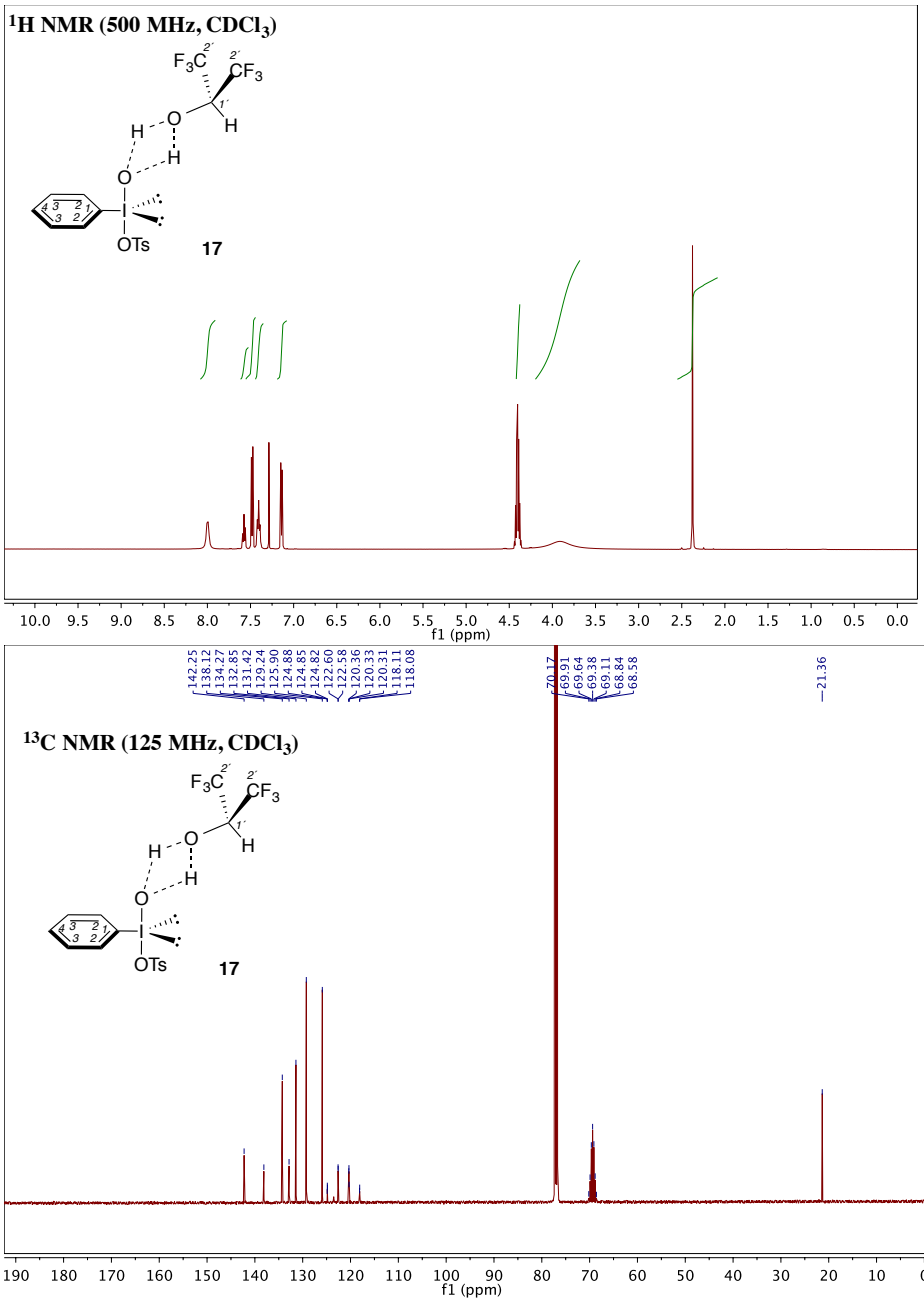


4.8. ^{1}H and ^{13}C NMR of a 1:1 mixture of HFIP:HTIB (17).

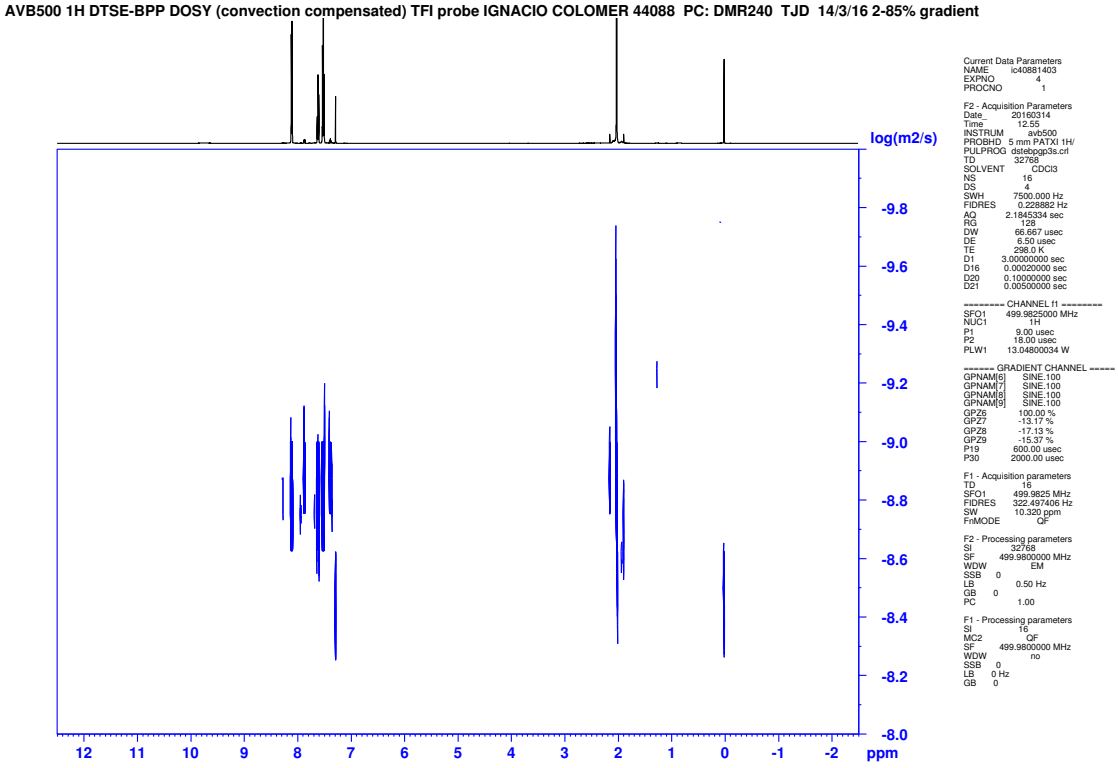


17

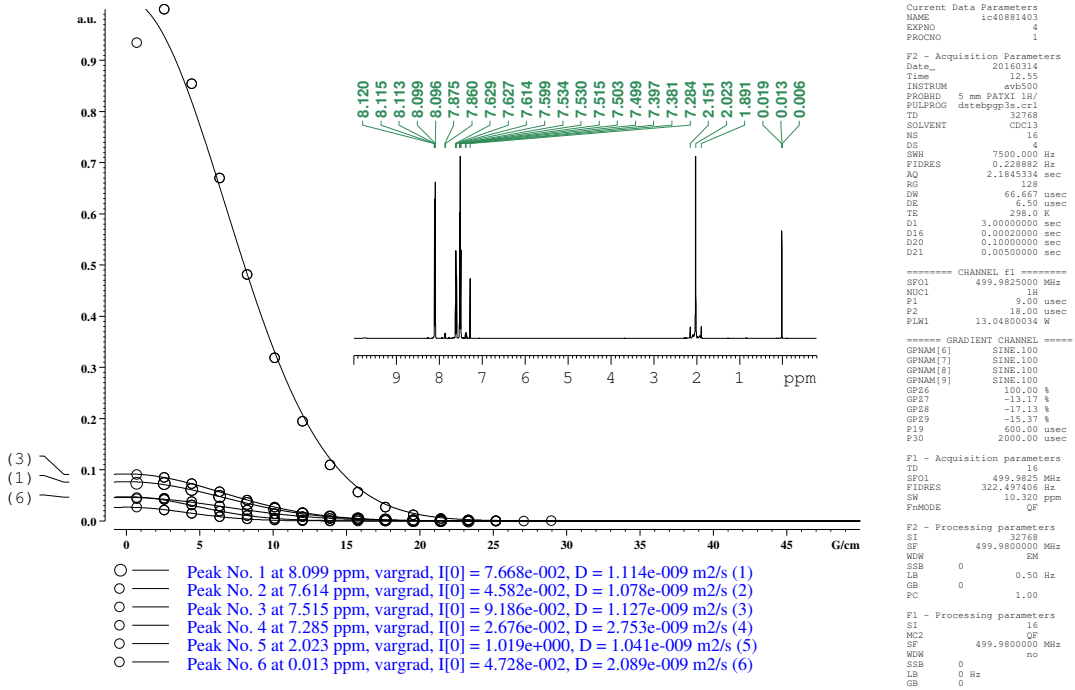
Data for **17**: **^{1}H NMR (500 MHz)** 8.00 (2 H, d, J = 7.8 Hz, 2-H), 7.58 (1 H, t, J = 7.5 Hz, 4-H), 7.48 (1 H, d, J = 8.2 Hz, 2 x CH Ts), 7.41 (2 H, t, J = 7.8 Hz, 3-H), 7.14 (2 H, d, J = 8.0 Hz, 2 x CH Ts), 4.40 (1 H, sept, $J_{H\text{-}F}$ = 6.0 Hz, 1´-H), 3.91 (1 H, br s, OH), 2.38 (3 H, s, Me Ts). **^{13}C NMR (125 MHz)** δ 142.3 (C Ts), 138.1 (C Ts), 134.3 (C-2), 132.9 (C-4), 131.4 (C-3), 129.2 (2 x CH Ts), 125.9 (2 x CH Ts), 123.5 (C-1), 121.5 (1C, qq, $J_{C\text{-}F}$ = 283.1 and 3.3 Hz, C-6), 69.4 (1 C, sept, $J_{C\text{-}F}$ = 33.3 Hz, C-1´), 21.4 (Me Ts).



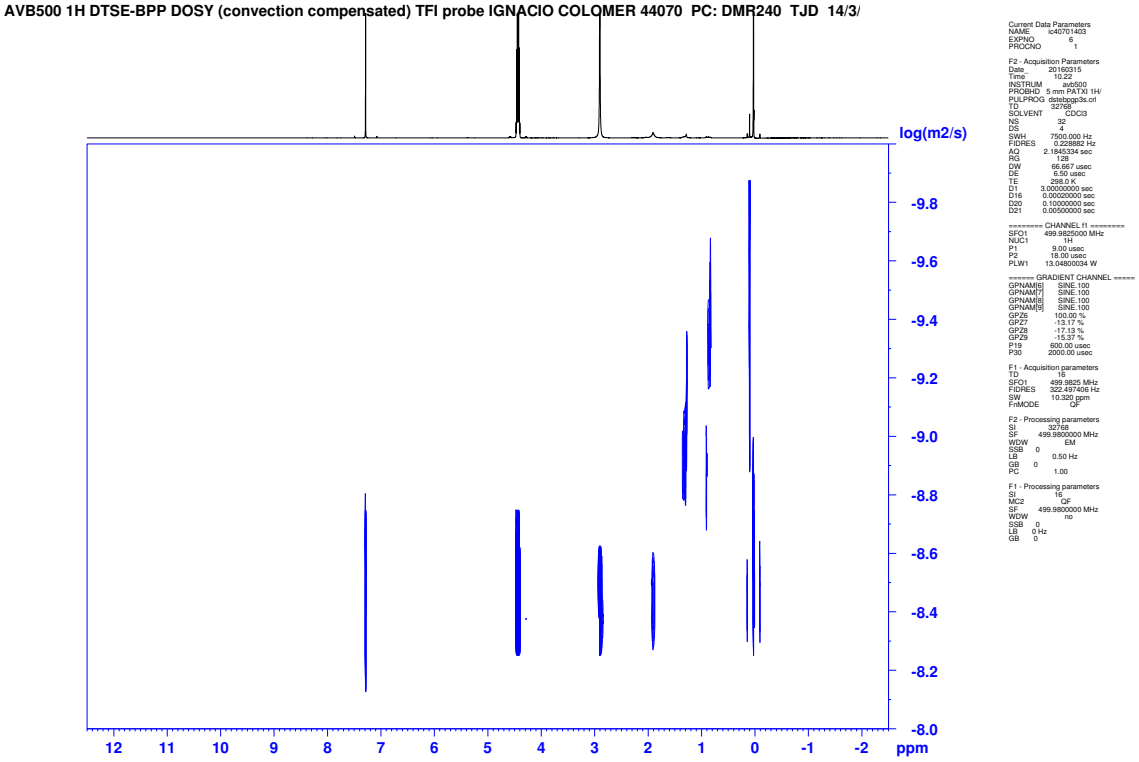
4.9. ^{1}H DOSY and Diffusion coefficient of PIDA (2).



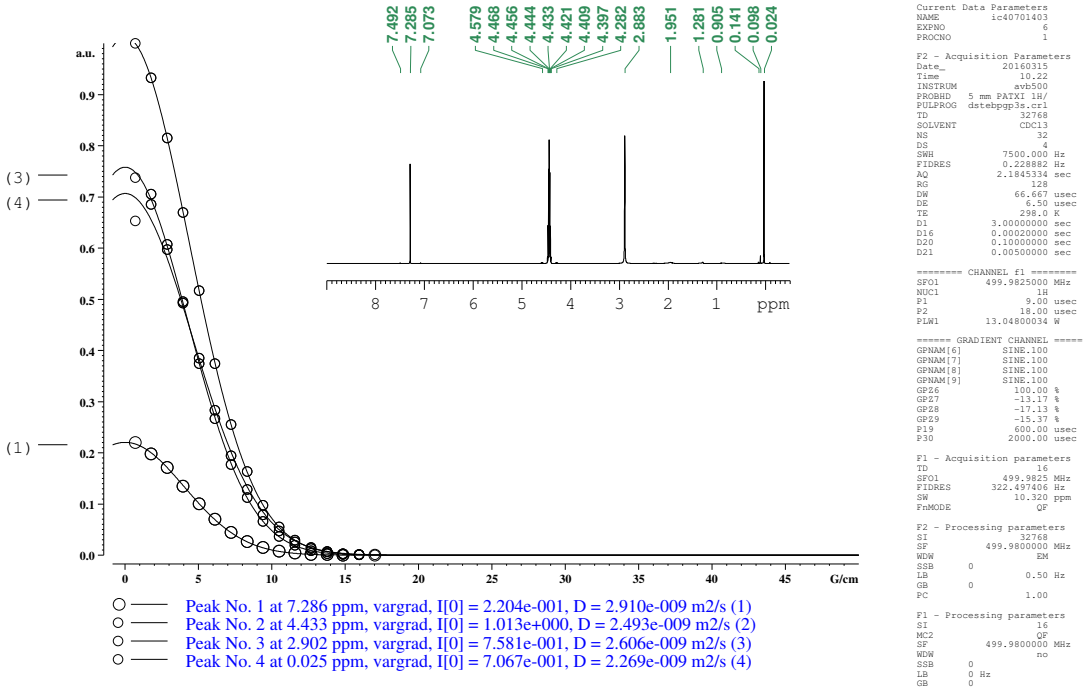
AVB500 1H DTSE-BPP DOSY (convection compensated) TFI probe IGNACIO COLOMER 44088 PC: DMR240 TJD 14/3/16 2-85% gradient



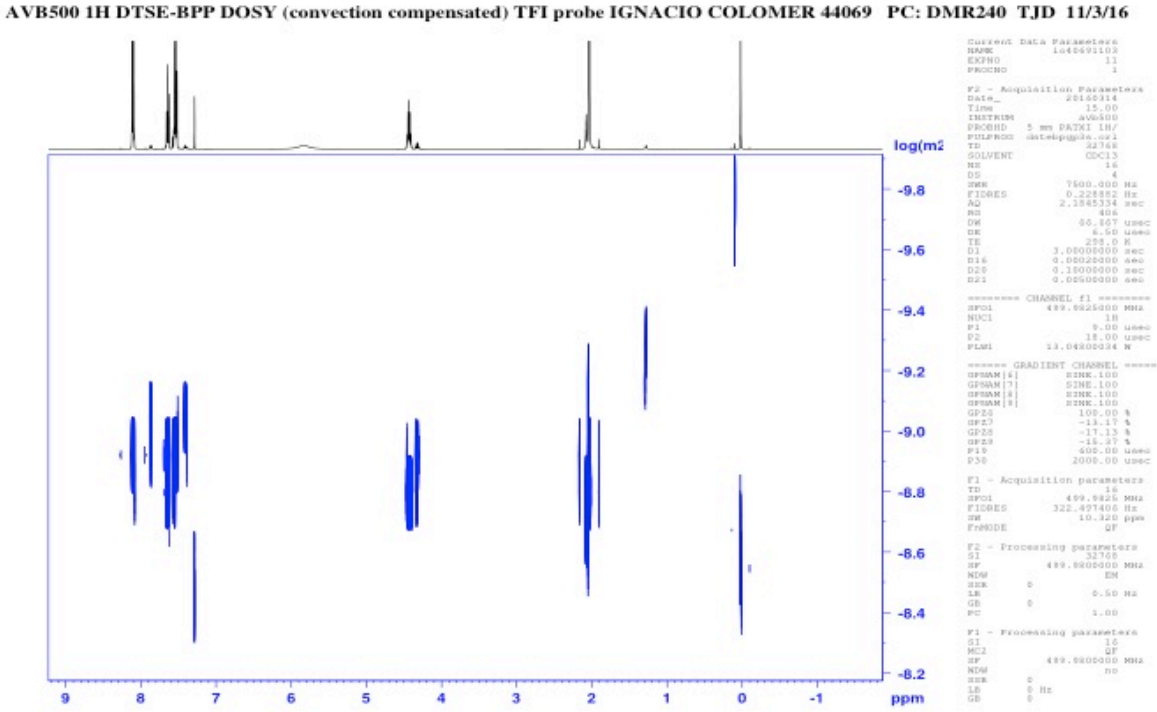
4.10. ^{1}H DOSY and Diffusion coefficient of HFIP (3).

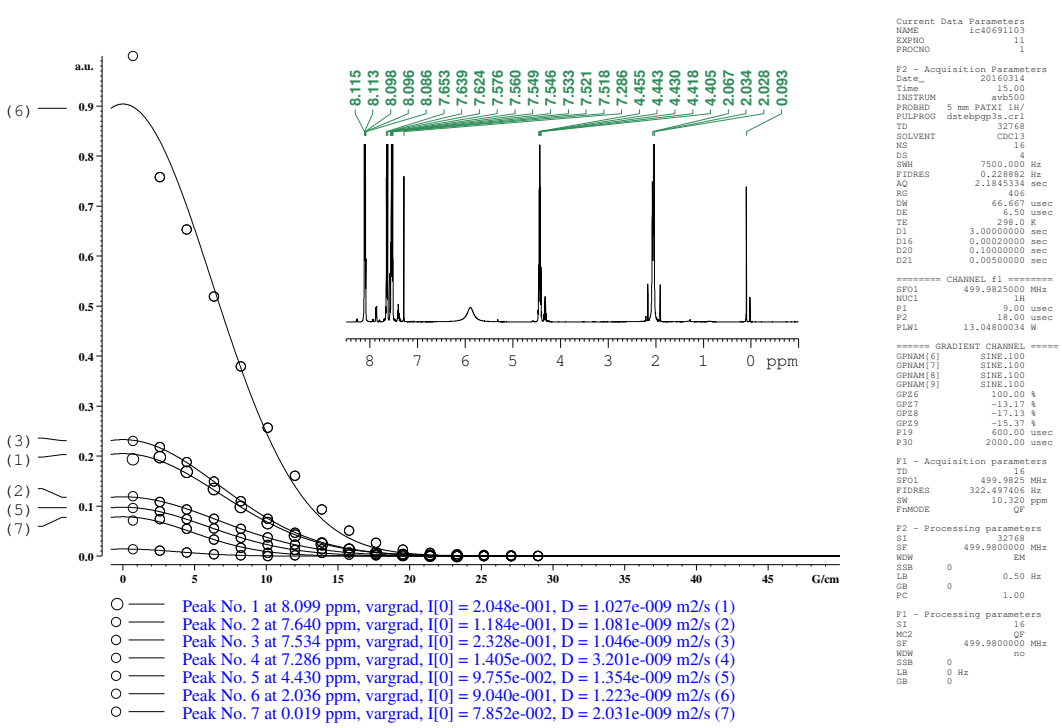


AVB500 1H DTSE-BPP DOSY (convection compensated) TFI probe IGNACIO COLOMER 44070 PC: DMR240 TJD 14/3/16 2-85% gradient



4.11. ^{1}H DOSY and Diffusion coefficient of a 1:1 mixture of HFIP:PIDA (5).





Current Data Parameters
NAME 1c40691103
EXPNO 11
PROCNO 1

F2 - Acquisition Parameters
Date_ 20160314
Time 15.00
INSTRUM avb500
PROBHD 5 mm PATXI 1H/
PULPROG dstebpgp3s.cr1
TD 32768
SOLVENT CDCl3
NS 16
DS 4
SWH 7500.000 Hz
FIDRES 0.228882 Hz
AQ 2.1845334 sec
RG 406
DW 66.667 usec
DE 6.50 usec
TE 298.0 K
D1 3.00000000 sec
D16 0.00020000 sec
D20 0.10000000 sec
D21 0.00500000 sec

======== CHANNEL f1 ========
SFO1 499.9825000 MHz
NUC1 1H
P1 9.00 usec
P2 18.00 usec
PLW1 13.04800034 W

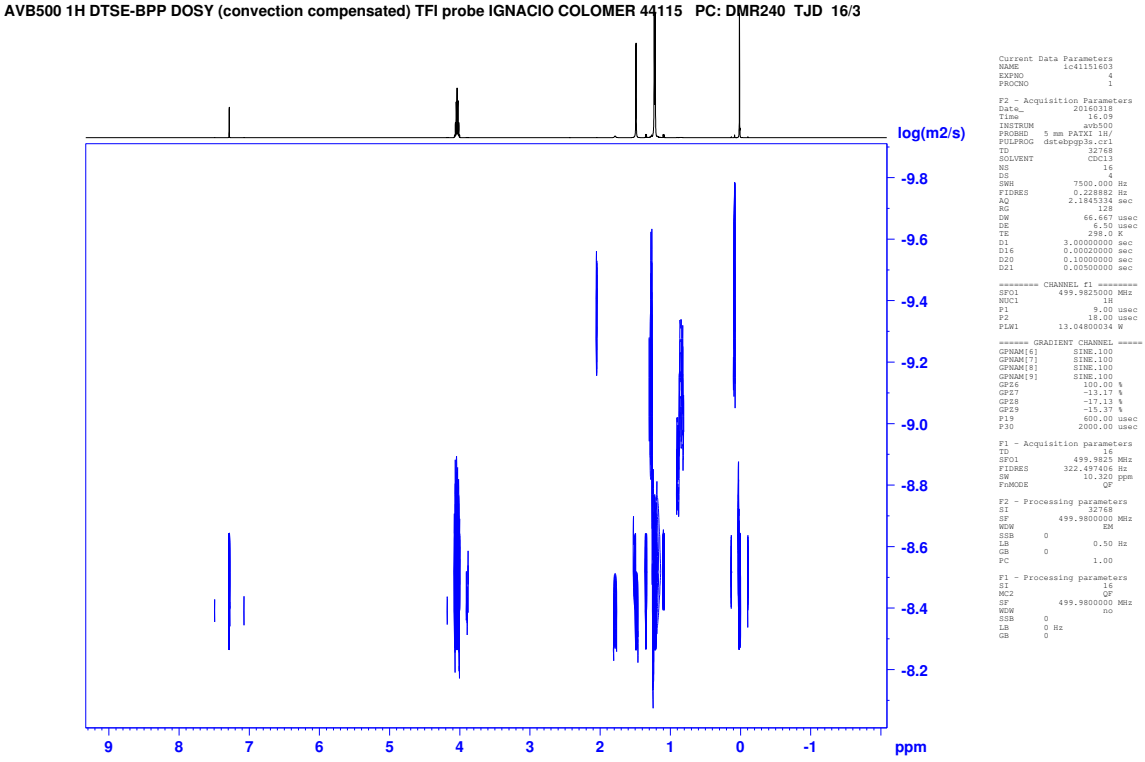
====== GRADIENT CHANNEL =====
GPNAM[6] SINE.100
GPNAM[7] SINE.100
GPNAM[8] SINE.100
GPNAM[9] SINE.100
GPZ6 100.00 %
GPZ7 -13.17 %
GPZ8 -17.13 %
GPZ9 -15.37 %
P19 600.00 usec
P30 2000.00 usec

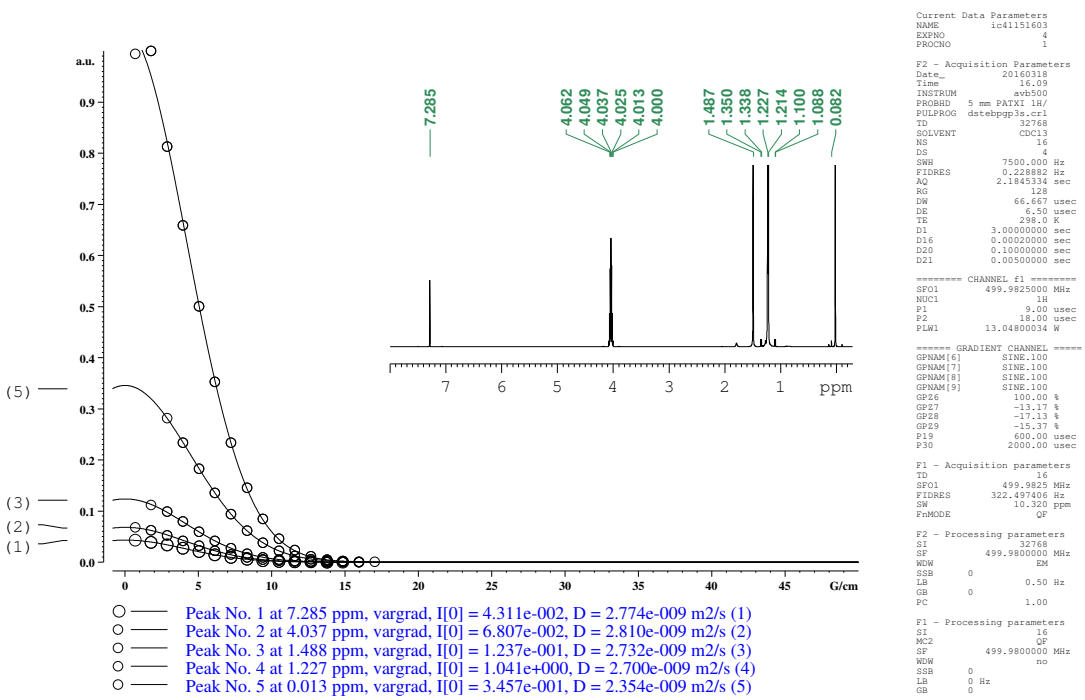
F1 - Acquisition parameters
TD 16
SFO1 499.9825 MHz
FIDRES 322.497406 Hz
SW 10.320 ppm
FnMODE QF

F2 - Processing parameters
SI 32768
SF 499.9800000 MHz
WDW EM
SSB 0
LB 0.50 Hz
GB 0
PC 1.00

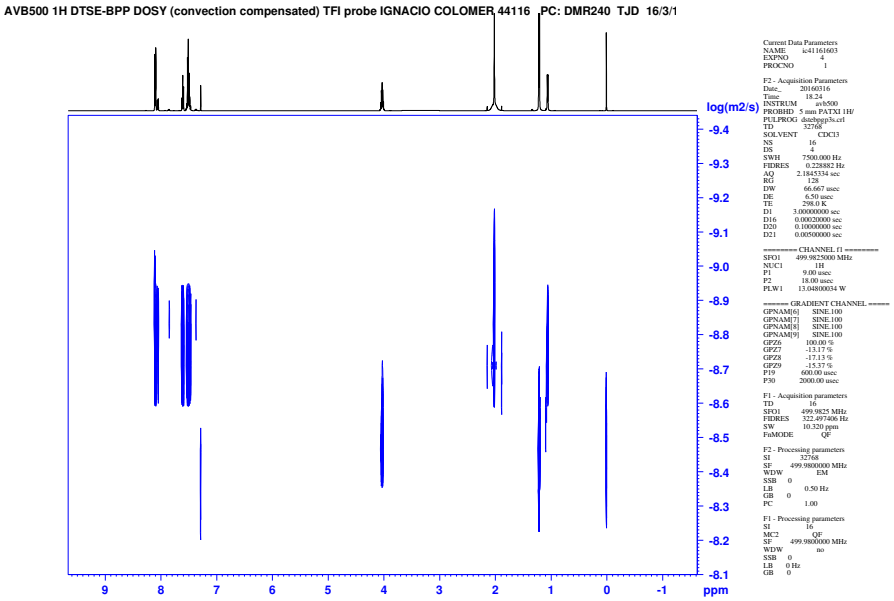
F1 - Processing parameters
SI 16
MC2 QF
SF 499.9800000 MHz
WDW no
SSB 0
LB 0 Hz
GB 0

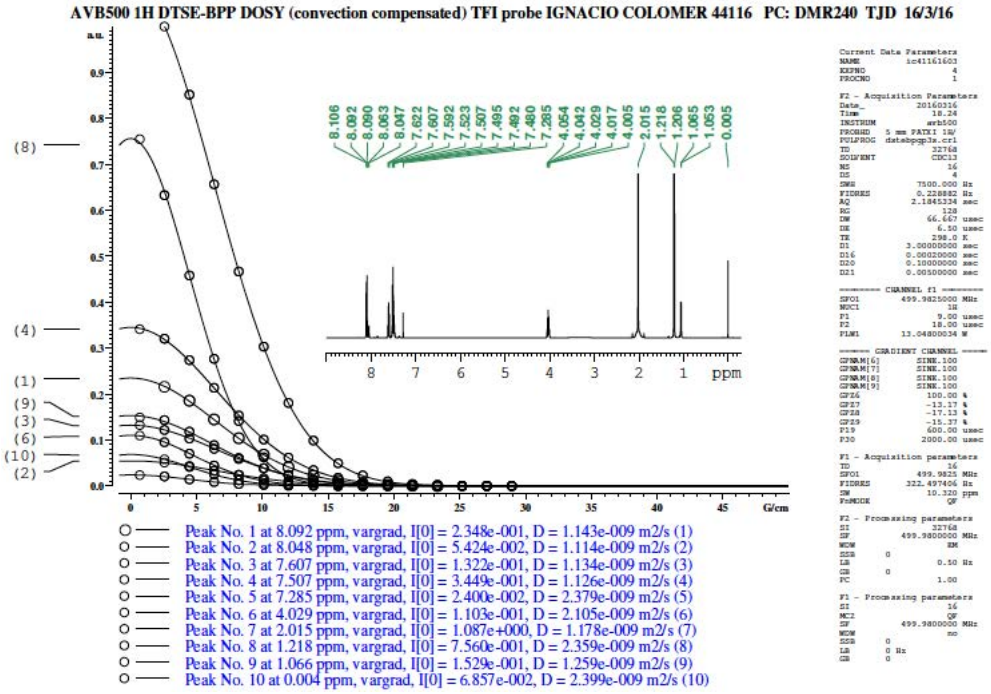
4.12. DOSY and Diffusion coefficient of *i*-PrOH





4.13. ^{1}H DOSY and Diffusion coefficient of a 1:1 mixture of *i*-PrOH:PIDA (18).

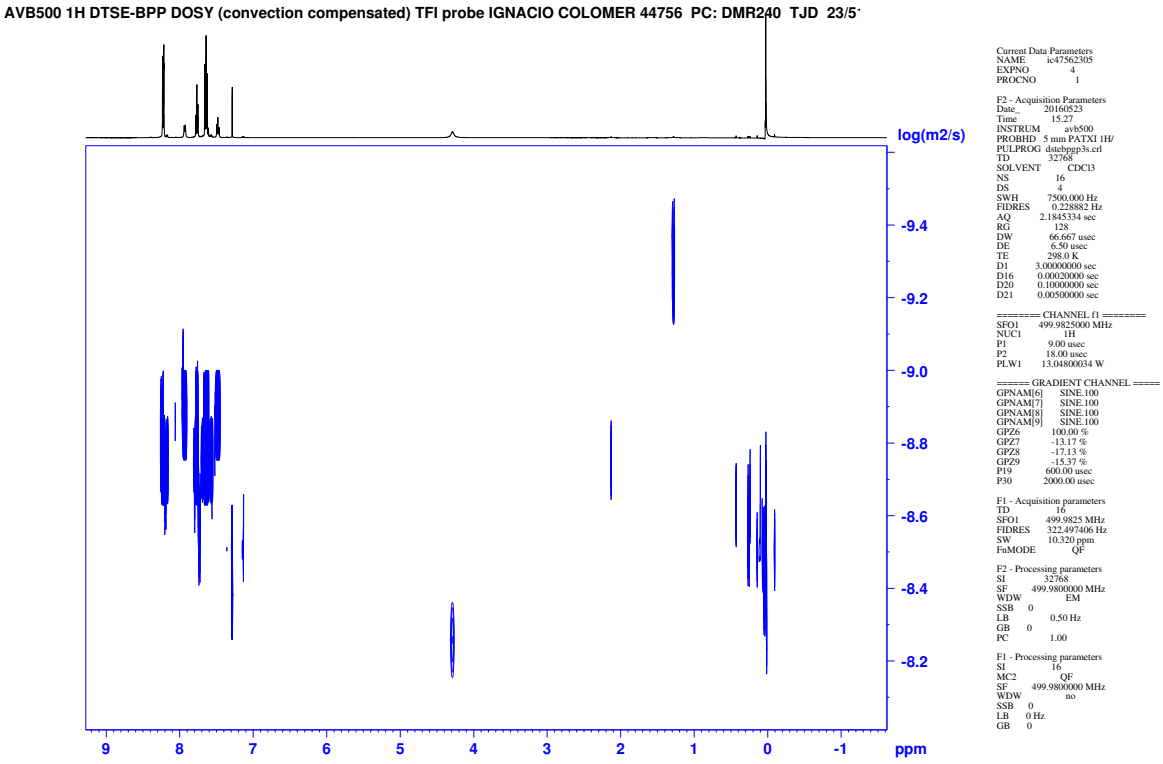




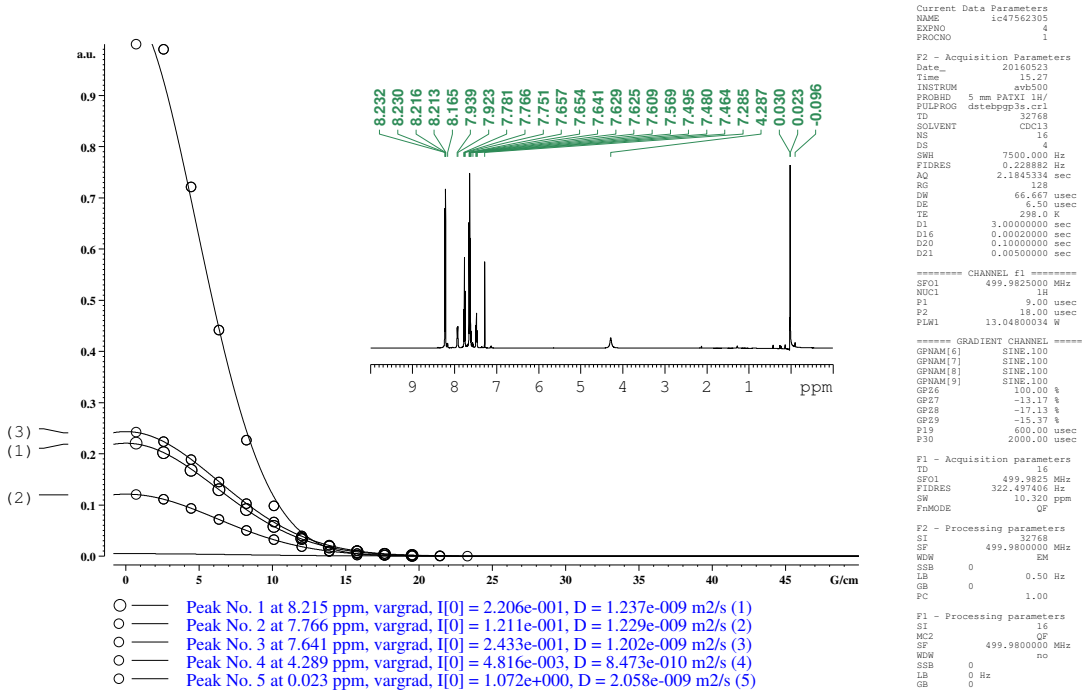
4.14. Table 1: Diffusion coefficients of PIDA (2), *i*-PrOH and the 1:1 mixture of PIDA: *i*-PrOH (18) in $CDCl_3$ as measured via DOSY

Compound	D (10^{-9} m^2 s^{-1})	D / D^{TMS}
TMS	2.13	1.00
2	1.09	0.52
***i*-PrOH**	2.49	1.10
18 (PIDA)	1.15	0.54
18 (*i*-PrOH)	2.23	1.05

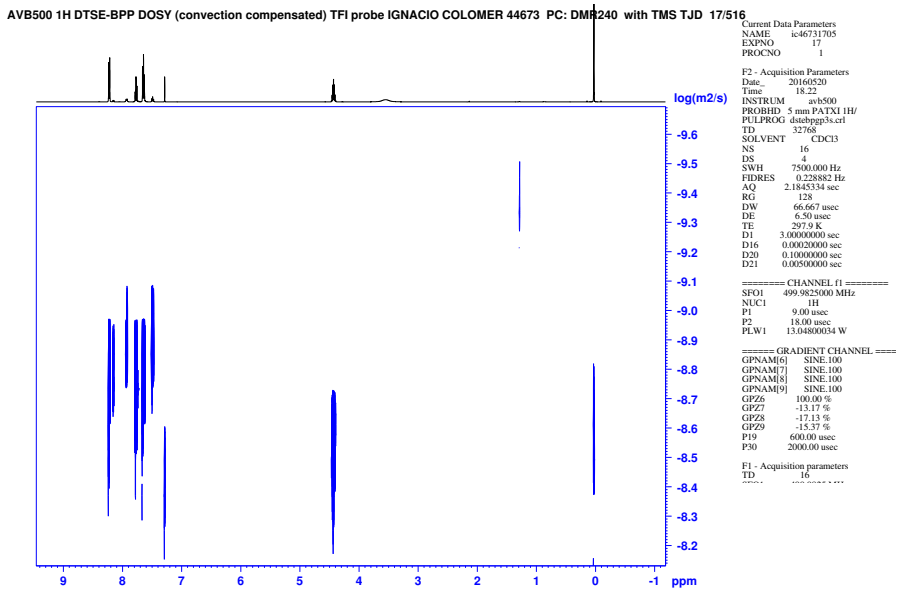
4.15. ^{1}H DOSY and Diffusion coefficient of PIFA

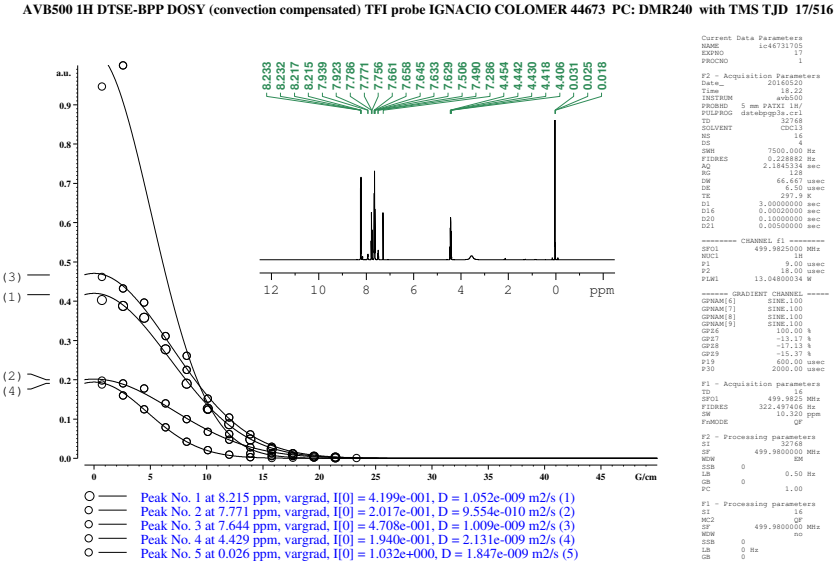


AVB500 1H DTSE-BPP DOSY (convection compensated) TFI probe IGNACIO COLOMER 44756 PC: DMR240 TJD 23/516



4.16. ^{1}H DOSY and Diffusion coefficient of a 1:1 mixture of HFIP:PIFA (16).

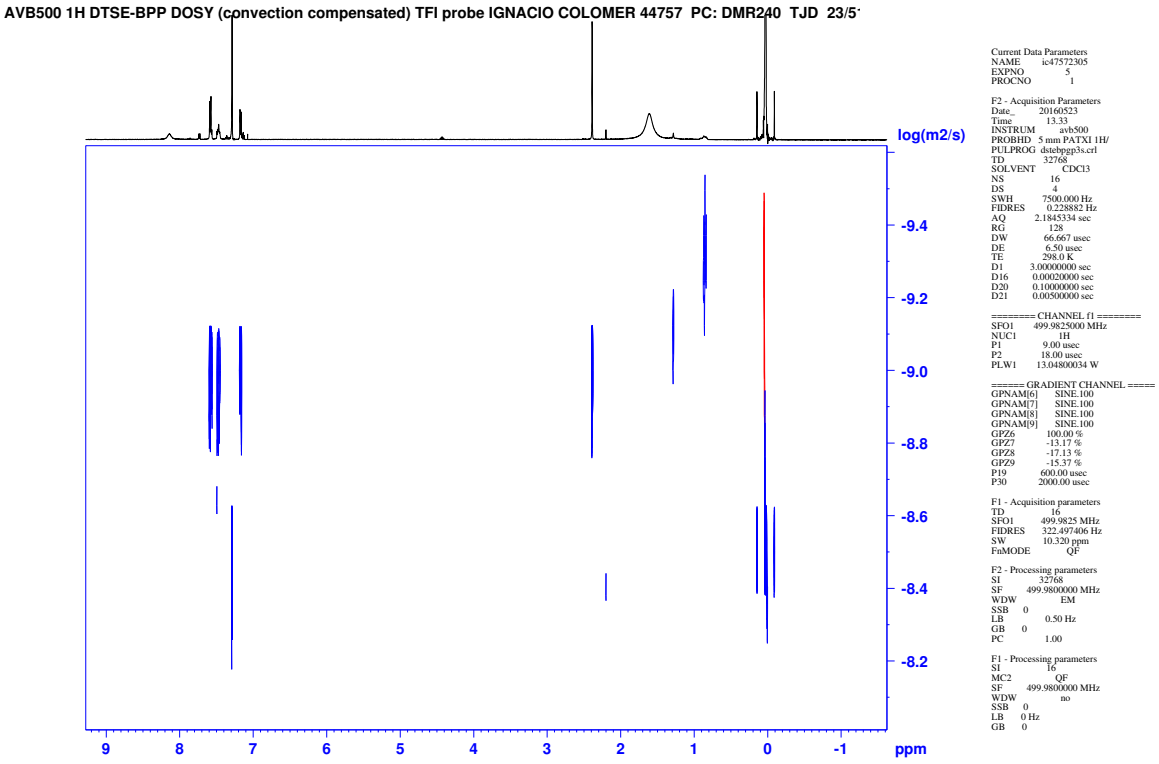




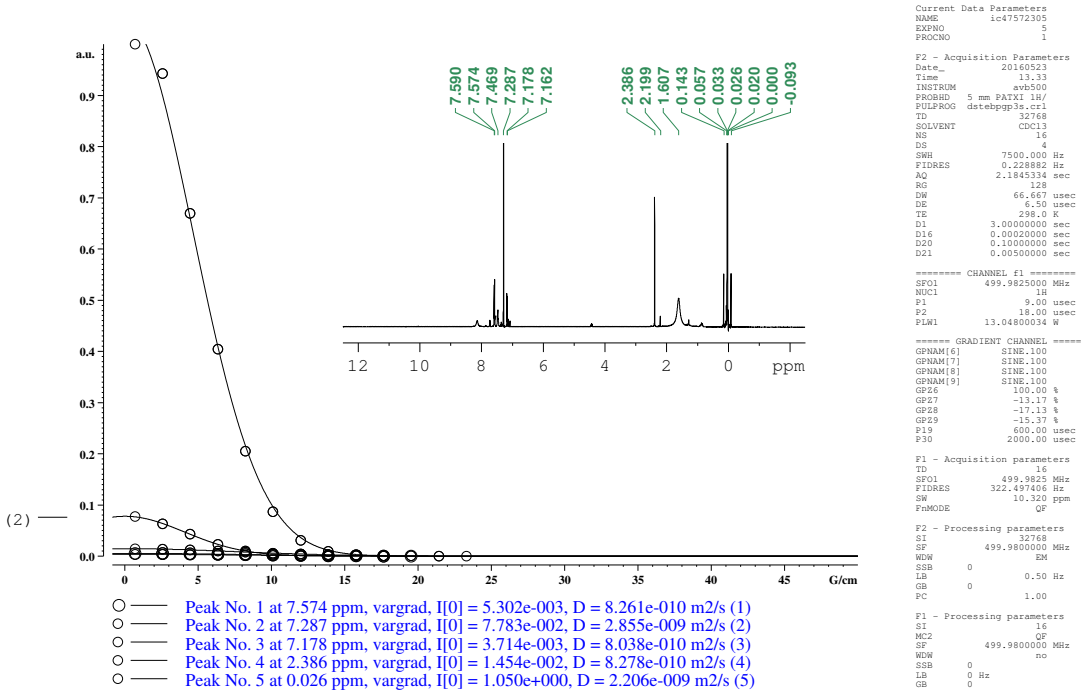
4.17. Table 2: Diffusion coefficients of PIFA, HFIP and the 1:1 mixture of PIFA:HFIP (16) in $CDCl_3$ as measured via DOSY

Compound	D (10^{-9} m^2 s^{-1})	D / D^{TMS}
TMS	2.06	1.00
HFIP	2.49	1.10
PIFA	1.22	0.59
16 (HFIP)	2.10	1.05
16 (PIFA)	1.05	0.63

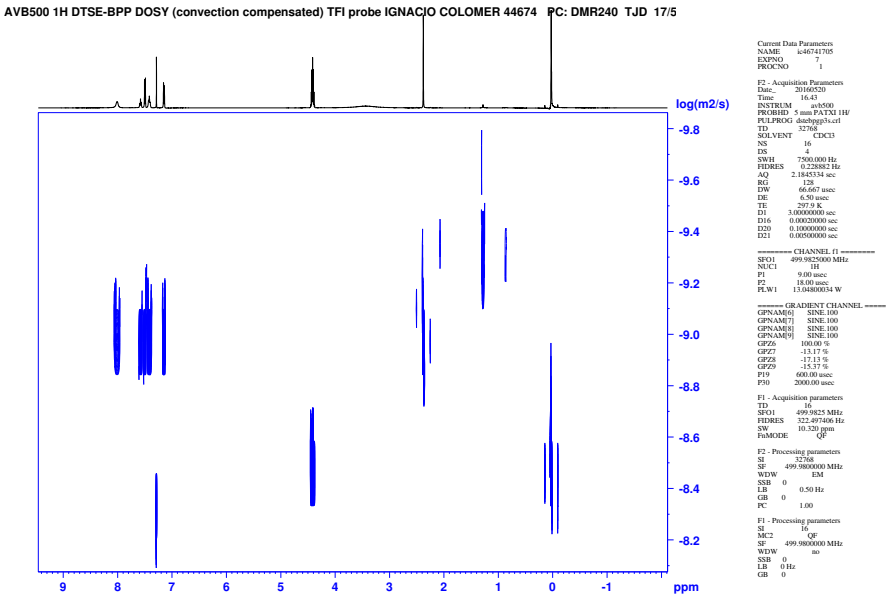
4.18. ^{1}H DOSY and Diffusion coefficient of HTIB

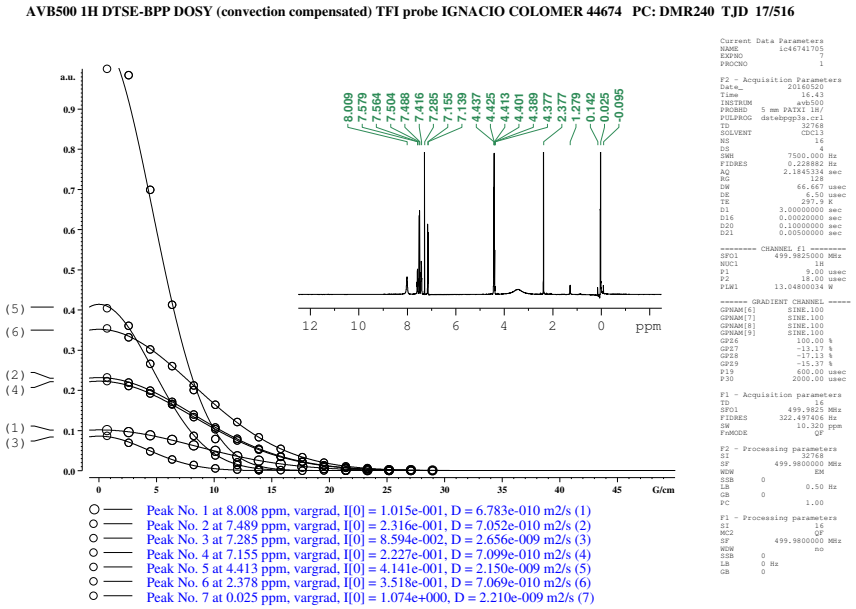


AVB500 1H DTSE-BPP DOSY (convection compensated) TFI probe IGNACIO COLOMER 44757 PC: DMR240 TJD 23/516



4.19. ^{1}H DOSY and Diffusion coefficient of a 1:1 mixture of HFIP:HTIB (17).





4.20. Table 3: Diffusion coefficients of HFIP, HTIB and the 1:1 mixture of HFIP: HTIB (17) in $CDCl_3$ as measured via DOSY

Compound	D (10^{-9} m^2 s^{-1})	D / D^{TMS}
TMS	2.21	1.00
HFIP	2.49	1.10
HTIB	0.82	0.37
17 (HFIP)	2.15	0.97
17 (HTIB)	0.71	0.32

5. References

[1] Colomer, I.; Coura Barcelos, R.; Donohoe, T. J. *Angew. Chem. Int. Ed.* **2016**, *55*, 4748-4752.
[2] Yu, J.; Gaunt, M. J.; Spencer, J. B. *J. Org. Chem.* **2002**, *67*, 4627.
[3] (a) Banks, C. E.; Compton, R. G. Understanding Voltammetry 2nd Ed. **2010** World Scientific.
[4] (a) Guidelli, R.; Compton, R.G.; Feliu, J. M.; Gileadi, E.; Lipkowski, J.; Schmickler, W.; Trasatti, S. *Pure Appl. Chem.* **2014**, 86, 245–258. (b) Guidelli, R.; Compton, R.G.; Feliu, J. M.; Gileadi, E.; Lipkowski, J.; Schmickler, W.; Trasatti, S. *Pure Appl. Chem.* **2014**, 86, 259–262.
[5] Demaille, C.; Bard, A. J. *Acta Chem. Scand.* **1999**, 53, 842-848.